

文章编号: 0258-7106 (2023) 06-1101-20

Doi: 10.16111/j.0258-7106.2023.06.002

湘东南东风岩体锆石 U-Pb 年代学、Hf 同位素组成 及稀土矿床特征^{*}

张锦煦¹, 林碧海¹, 廖凤初², 孙骥¹, 谭仕敏¹, 何艳林², 周超¹, 朱继华¹,
熊雄¹, 李超¹, 陈剑锋^{1, 2, 3**}

(1 湖南省地质调查所,湖南长沙 410116; 2 湖南省地球物理地球化学调查所,湖南长沙 410116; 3 中南大学有色金属成
矿预测与地质环境监测教育部重点实验室,湖南长沙 410083)

摘要 文章对湘东南地区的东风岩体进行了锆石 LA-ICPMS U-Pb 年龄、Hf 同位素以及岩石地球化学分析,以研究岩石成因及形成构造背景,并对东风风化壳离子吸附型重稀土矿的成因进行了探讨。东风岩体 2 件二长花岗岩的锆石 U-Pb 年龄为(433.5±2.6)Ma 和(432.0±2.5)Ma,显示为加里东晚期。东风岩体锆石 $\epsilon_{\text{Hf}}(t)$ 值介于-5.12~7.45,计算得到二阶段地幔亏损模式年龄(T_{DM2})介于 1714~1882 Ma,显示其成岩物质为壳源的特征。东风岩体的地球化学特征显示其为高钾钙碱性、强过铝质的花岗岩,在成因类型判别图解中显示为 S 型花岗岩,构造背景判别图解显示为后碰撞构造环境。综合东风岩体花岗岩的地球化学特征和 Hf 同位素特征,笔者认为,东风岩体形成于扬子板块与华夏板块陆内汇聚的后碰撞伸展环境,为增厚地壳减压熔融和软流圈地幔上涌诱发古老地壳物质重熔形成的 S 型花岗岩。东风稀土矿床为一个由富轻稀土元素的母岩经风化后形成的大型重稀土矿床,富含稀土元素的高 Y 型花岗岩母岩为矿床的形成提供了重要物质基础,气候及地形地貌条件为稀土元素发生淋滤迁移和吸附富集提供了重要保证。

关键词 东风花岗岩体; 加里东期; 锆石 U-Pb 定年和 Hf 同位素; 离子吸附型稀土矿; 矿床成因; 湘东南
中图分类号:P618.7 **文献标志码:**A

Zircon U-Pb chronology, Hf isotopes and REE deposit characteristics of Dongfeng granitic pluton in southeastern Hunan Province

ZHANG JinXu¹, LIN BiHai¹, LIAO FengChu², SUN Ji¹, TAN ShiMin¹, HE YanLin², ZHOU Chao¹, ZHU JiHua¹,
XIONG Xiong¹, LI Chao¹ and CHEN JianFeng^{1, 2, 3}

(1 Geological Survey Institute of Hunan Province, Changsha 410116, Hunan, China; 2 Geophysical and Geochemical Survey
Institute of Hunan, Changsha 410116, Hunan, China; 3 Key Laboratory of Metallogenesis Prediction of Nonferrous Metals and
Geological Environment Monitoring, Ministry of Education, Central South University, Changsha 410083, Hunan, China)

Abstracts

This paper presents new zircon LA-ICP-MS U-Pb ages, Lu-Hf isotope and geochemical data of the Dongfeng granitic pluton in southeastern part of Hunan Province, aiming to constrain its petrogenesis and tectonic implication, and to explore the metallogenetic mechanism of the Dongfeng ion adsorption type heavy rare-earth deposit. The LA-ICP-MS zircon U-Pb analysis of two biotite monzogranite yielded $^{206}\text{Pb}/^{238}\text{U}$ ages of (433.5±2.6)Ma and

* 本文得到中国地质调查局二级项目(编号:DD20230055、12120115029301)、湖南省地质院科研项目(编号:HNGSTP202306)和湖南省自然资源厅科研项目(编号:2023-02)联合资助

第一作者简介 张锦煦,男,1982 年生,硕士,高级工程师,从事地质找矿与研究工作。Email: 609126729@qq.com

** 通讯作者 陈剑锋,男,1985 年生,博士,高级工程师,从事地质找矿与研究工作。Email: chenjianfeng021041@163.com

收稿日期 2023-05-11; 改回日期 2023-10-25。秦思婷编辑。

(432.0 ± 2.5) Ma, respectively, suggesting that the Dongfeng granitic pluton formed in Late Caledonian. The granites contain high K₂O and belong to calc-alkali, strongly peraluminous ($A/CNK=1.12\sim1.43$), and geochemically classified as S-type granite. The primitive mantle-normalized trace element spider diagram shows that the Dongfeng monzogranite is relatively depleted in Ba, Nb, Sr, P, Ti and relatively enriched in Rb, (Th+U), Nd, (Zr+Hf) as well as zircon $\varepsilon_{\text{Hf}}(t)$ (-5.12 to -7.45) and $^{176}\text{Hf}/^{177}\text{Hf}$ (0.282 300 to 0.282 374) values indicating that this pluton is mostly product of crust melting. Tectonic setting discrimination diagrams show characteristics of monzogranite produced in post-collisional extensional environment. Hf isotopic and geochemical analyses indicate that the Dongfeng monzogranite belongs to S-type granite, derived from the partial melting of old crustal materials, when asthenosphere mantle upwelling, causing remelting of crustal materials under the geodynamical background of extensional environment after intraplate convergence between Yangtze Plate and Cathaysia Plate. The Dongfeng deposit is a newly discovered, large-sized ion adsorption type heavy rare-earth deposit, with an averaging grade of 0.050%~0.099% of REO, which formed from weathering of biotite monzogranite enriched in LREE, the high content of Y in parent granite provides the major sources in the formation of the deposit. Topographic features and climatic characteristics in the Dongfeng area are the key conditions for eluviation and sorption inducing the formation of ion adsorption type rare-earth deposit.

Key words: Dongfeng granitic pluton, Caledonian, zircon U-Pb geochronology and Hf isotope, ion adsorption type rare-earth deposit, ore genesis, southeastern Hunan Province

湘东南地区地处南岭中段,位于华夏地块与扬子地块结合部位的东侧(图1a),区域NE向茶陵—郴州大断裂从区内通过(图1b)。区内多时代的花岗岩及其成矿作用长期以来为地质学者研究的重点,前人已对区内花岗岩地球化学特征及其侵位年龄、构造背景、成矿作用等进行了深入研究,特别是在年代学方面积累了较多的数据,如张文兰等(2011)获得彭公庙岩体的LA-ICP-MS 锆石U-Pb年龄436.2~435.3 Ma,与程顺波等(2013)获得该岩体锆石SHRIMP U-Pb年龄(441.1 ± 3.1) Ma比较吻合,证实其形成于加里东期;Wang等(2007a)获得五峰仙岩体的LA-ICP-MS 锆石U-Pb年龄为(236.0 ± 6) Ma,与陈迪等(2017)获得的(233.5 ± 2.5) Ma的锆石SHRIMP U-Pb年龄在误差内一致,表明其形成于印支期;锡田岩体的锆石U-Pb年龄显示其有印支期和燕山期花岗岩,其中印支期花岗岩的侵位时限为225~220 Ma(陈迪等,2013;姚远等,2013;Liang et al., 2016; Wu et al., 2016),燕山期花岗岩为155~150 Ma(马铁球等,2005;陈迪等,2013;周云等,2013;牛睿等,2015;Zhou et al., 2015; Liang et al., 2016);万洋山岩体和诸广山北体均有加里东期、印支期和燕山期的花岗岩出露(伍光英等,2008;陈迪等,2016;郭爱民等,2017)。受多时代花岗岩浆活动的影响,该区发生了大规模多金属成矿作用。东风岩体位于该区茶陵—郴州大断裂东侧、彭公庙岩体与万洋山岩体之

间(图1b),走向近南北,长约15 km,东西宽约3 km,出露面积43 km²。岩体西侧侵入于寒武系—奥陶系浅变质砂岩、板岩中,东部与泥盆系跳马涧组石英砂岩呈沉积接触(图1c),据此可推断其应为加里东期岩体,但缺乏准确的年龄数据。

湘东南所在南岭地区不仅是中国钨锡等有色金属的富集地,也是中国离子吸附型稀土矿的矿集区(王登红等,2013),近年来湖南省地调院在该区开展了区域性找矿工作,在万洋山、彭公庙、东风岩体内陆续新发现了一批如青广坪、塘窝、白面石、牛头坳、东风等稀土矿床(点)(图1b),经初步调查评价,这些矿床(点)均具备寻找中大型离子吸附型稀土矿的潜力(湖南省地质调查院,2014;2018)。离子吸附型稀土矿床可分为轻稀土矿床和重稀土矿床,一般认为稀土矿的成矿作用对母岩的稀土元素成分具有明显的继承性(周美夫等,2020),表现为重稀土矿在相对富重稀土元素的母岩中富集,而轻稀土矿的母岩则具有相对富轻稀土元素的特征(Li et al., 2017)。而本文的研究显示,该区东风岩体内的东风稀土矿床则为一由富轻稀土元素的花岗岩作为母岩经风化后形成的重稀土矿床,其成矿作用研究对丰富稀土成矿理论及拓宽重稀土矿的找矿方向具有重要意义。

笔者在对东风岩体进行系统的岩石矿物学野外考察以及稀土矿含矿性调查基础上,获得2件花岗岩样品的锆石LA-ICPMS U-Pb年龄、Hf同位素数据

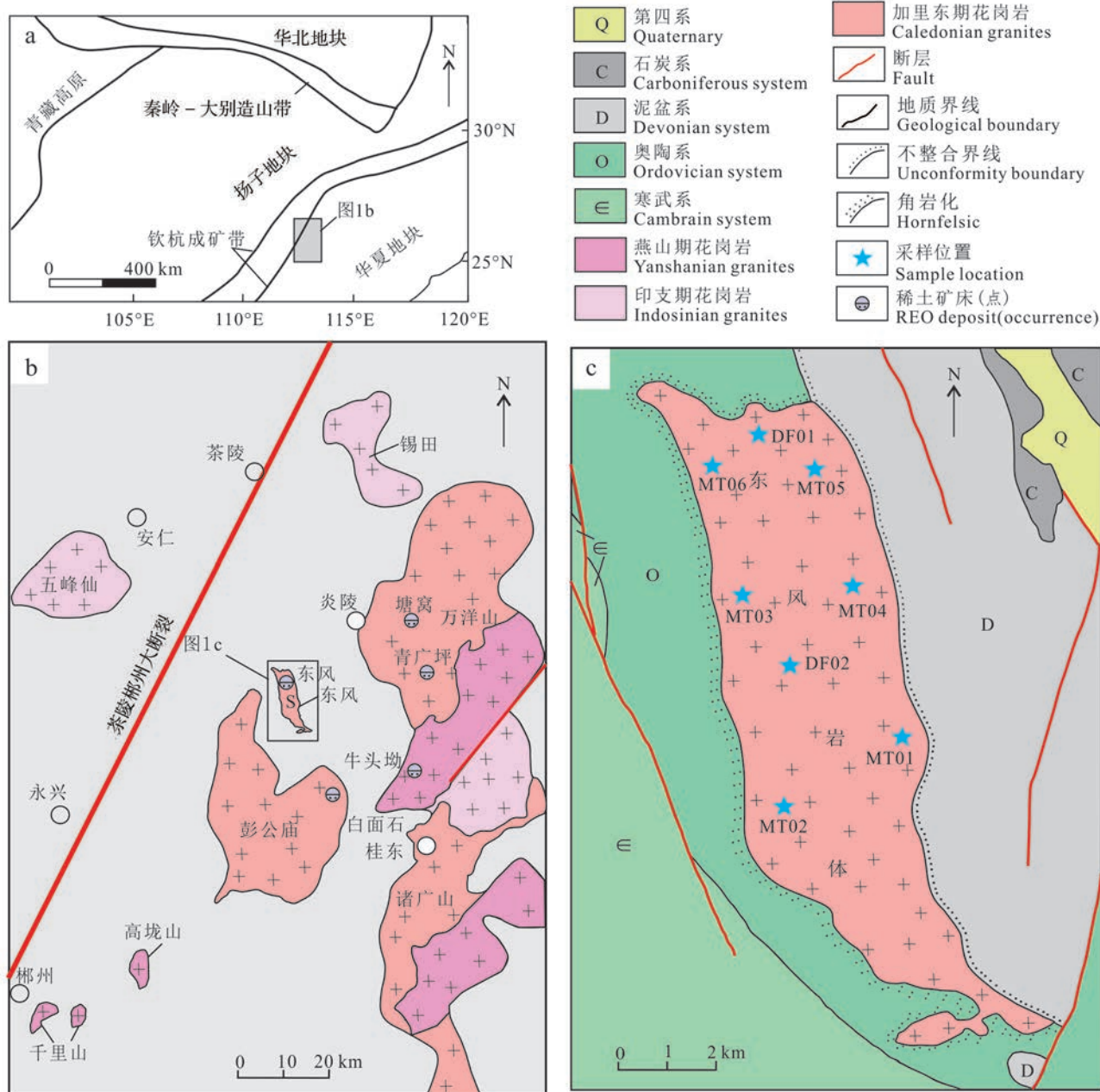


图1 湘东南地区大地构造位置简图(a)、花岗岩分布图(b)和东风岩体地质简图(c)(据柏道远等,2006修改)
Fig. 1 Geotectonic location (a), distribution of granitic plutons (b) in southeastern Hunan Province and geologic sketch of the Dongfeng pluton (c) (modified after Bai et al., 2006)

及一批地球化学数据,据此对东风岩体侵位时限、岩石成因、构造背景,以及东风稀土矿床的成矿特征等问题进行探讨。

1 岩体地质特征及含矿性特征

由原湖南省地质调查院在该区所完成的1:1万地质测量成果显示,与相邻彭公庙岩体、万洋山岩体

等大岩基内产出有大量晚期侵入的岩脉不同,东风岩体地表极少有石英脉和细晶岩脉出露,且岩体内未见有基性岩脉,其岩性单一,为粗中粒(少)斑状黑云母二长花岗岩。整个岩体地表风化严重(图2a),经浅井与浅钻工程揭露,其风化壳在垂向上可分为4层,即腐殖层、残坡积层、全风化层和半风化层(图3)。全风化层厚度基本大于10 m(山顶陡坎及河沟处除外),最厚部位约为38 m,呈土黄色或紫红色;腐

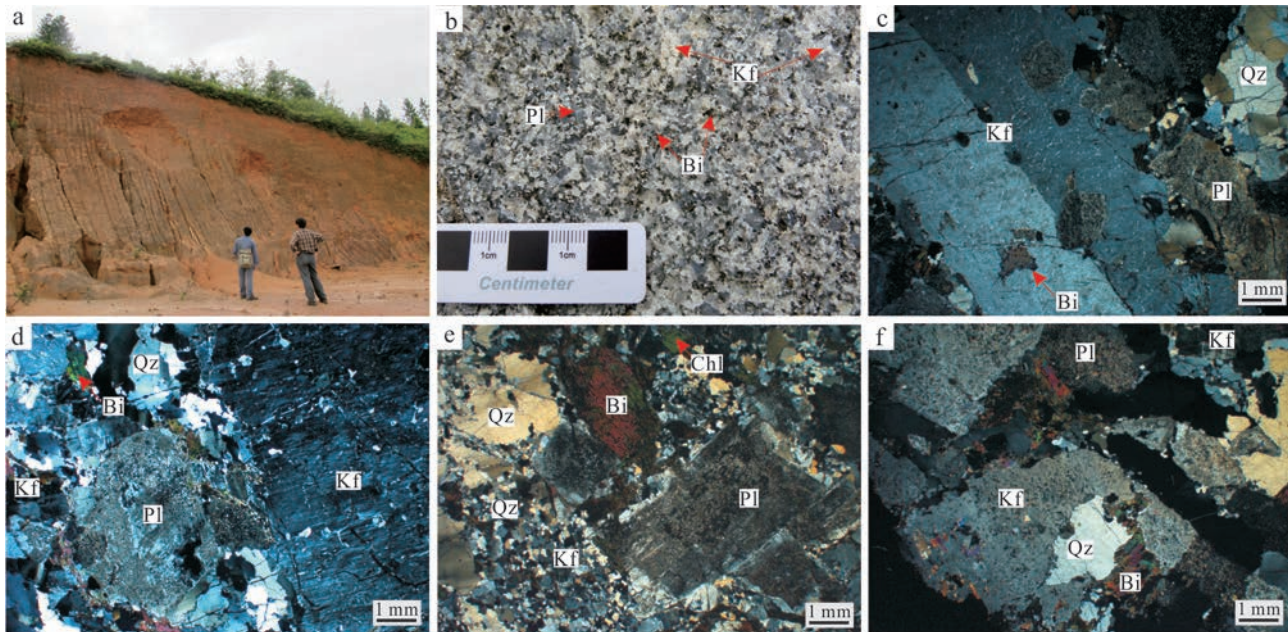


图2 东风岩体野外露头、岩石学特征和显微岩相学特征

a. 东风岩体野外露头;b. 花岗岩手标本照片;c. 钾长石斑晶具卡式双晶结构(+);d. 钾长石具条纹结构,斜长石绢云母化(+);e. 黑云母绿泥石化(+);f. 黑云母中的独居石和磷灰石(+)

Ap—磷灰石; Bi—黑云母; Chl—绿泥石; Kf—钾长石; Mnz—独居石; Pl—斜长石; Qz—石英; Ser—绢云母

Fig. 2 Photos of filed geology, petrological and micrograph of the Dongfeng pluton

a. Outcrop of the Dongfeng intrusive body; b. Hand specimen of granite; c. K-feldspar shows Carlsbad twin texture(+); d. K-feldspar shows stripe structure and plagioclase shows sericite-alteration(+); e. Chlorite altered biotite(+); f. Monazite and apatite coexisting with biotite(+)

Ap—Apatite; Bi—Biotite; Chl—Chlorite; Kf—Feldspar; Mnz—Monazite; Pl—Plagioclase; Qz—Quartz; Ser—Sericite

殖层和残坡积层厚度较小,一般在2~4 m左右,山顶部位不足2 m,甚至小于1 m;半风化层厚度不清。

在地表极少部位(河流中)见有未(弱)风化基岩,其岩性为粗中粒(少)斑状黑云母二长花岗岩,灰白色,粗中粒结构和似斑状结构,块状构造(图2b)。斑晶含量约占3%~8%,成分以钾长石为主,石英次之。基质矿物组成主要为钾长石(25%~35%)、斜长石(20%~35%)、石英(22%~30%)和黑云母(5%~10%),副矿物主要有独居石、磷灰石、榍石、锆石等。花岗岩蚀变十分普遍,多见有高岭土化、绿泥石化、钾长石化、绢云母化、硅化等。其中,钾长石化、高岭土化等与矿化关系密切。钾长石多呈半自形板状,具条纹结构,内部常包裹细粒石英、黑云母,斑晶常具有卡式双晶(图2c),基质见有格子双晶发育(图2d);斜长石多呈自形-半自形板状,多见聚片双晶,内部偶见有鳞片状绢云母化(图2d)等蚀变;石英为他形粒状,大者常具碎裂纹及波状消光(图2c~f),部分颗粒被长石侵蚀,具溶蚀港湾结构(图2e~f),另偶见细小(0.2~0.4 mm)等轴状石英呈锯齿状镶嵌集合

体产出(图2e),可能为受重结晶作用而成;黑云母呈片状或细片状集合体,部分蚀变形成绿泥石(图2e),显示蚀变残余结构,见与副矿物独居石、磷灰石等共生(图2f)。

东风风化壳离子吸附型稀土矿产于东风岩体内部,原湖南省核工业地质局301队对东风稀土矿普查时实施了钻探工程,见矿厚度一般4.50~12.00 m,最厚达20.9 m,REO品位0.050%~0.248%。在东风岩体内部圈定的多个稀土矿体规模较大,形态较好,矿体均呈层状赋存于花岗岩全风化层中(图3),产状与全风化层产状及地形坡向基本一致,倾角较地形坡角略平缓,其中单个矿体的平均厚度最大可达15 m,一般为4~8 m,矿体平均品位(REO)为0.052%~0.099%。对矿体所采集的多件样品测试显示,Y₂O₃的配分含量最高可达53.8%,平均为40.7%,表明稀土矿的矿化以重稀土元素为主。经资源储量估算,在探矿权范围内获得333+334类稀土(REO)资源量10.87万t,表明东风稀土矿的稀土远景资源量达到大型(湖南省核工业地质局三〇一大队,2018)。

分层	柱状图	厚度/m
腐殖层	≤ ≤ ≤ ≤ · · · ·	0.3~3.5
黏土层	- - - - - - - - - - - -	0.2~4.5
全风化层	+ // + // + - \\\n// + // + - \\\n\\ - \\ + // + -\n- \\ + \\ + \\ +\n+ // + // + - \\\n// + // + - \\\n\\ - \\ + // + -\n- \\ + \\ + \\ +\n+ // + // + - \\\n// + // + - \\\n\\ - \\ + // + -\n- \\ + \\ + \\ +\n+ // + // + - \\\n// + // + - \\\n\\ - \\ + // + -\n- \\ + \\ + \\ +\n+ // + // + - \\\n// + // + - \\\n\\ - \\ + // + -\n- \\ + \\ + \\ +	1.0~36.5
半风化层	\\\n- \\ + // + -\n- \\ + \\ + \\ +	不详

图 3 东风岩体风化壳柱状图

Fig. 3 Crust weathering profile of the Dongfeng pluton

2 样品分析测试

本次分析测试样品的采集位置见图 1b, 用于挑选锆石的样品 DF01 和 DF02 采集于新开公路陡坎花岗岩全风化层, 其中, 样品 DF01 采集于岩体北部边缘, DF02 采集于岩体中部位置; 用于主、微量元素分析的样品(MT01~06)为采集于切割较深河沟处的未遭受风化蚀变的新鲜花岗岩。

主、微量元素的分析测试在中国科学院地球化

学研究所矿床国家重点实验室完成,主量元素在 Axios(PW4400)型X射线荧光光谱仪中完成,测试精度优于3%;微量元素测试采用 Finnigan MAT公司生产的 ELEMENT 型高分辨等离子质谱仪完成。

锆石单矿物是在无污染的环境下用人工重砂方法初选(包括手工碎样、水洗、磁选),然后在双目镜下挑选,选出晶形较好、具代表性的锆石用环氧树脂充分固定、抛光,制成样品靶。锆石的CL图像和LA-ICPMS U-Pb定年在中国科学院地球化学研究所矿床地球化学国家重点实验室完成。

锆石 U-Pb 测试分析仪器为 PerkinElmer 生产的 ELAN DRC-e 型等离子质谱仪, 配套 GeoLasPro 193 nm 型准分子激光剥蚀系统, 所用束斑直径为 $32 \mu\text{m}$ 。原始测试数据用 ICPMSDataCal 软件进行处理 (Liu et al., 2008; 2010)。普通 Pb 校正方法参照 Andersen (2002), ^{206}Pb - ^{238}U 加权平均年龄和协和图解由 ISO-PLOT 软件获得 (Ludwig et al., 2003)。单个数据点误差均为 1σ 。

锆石 Hf 同位素分析在中国地质大学(武汉)GPMR 实验室 Neptune 多接收 MC-ICP-MS 仪器上进行。激光剥蚀所用斑束直径为 $44 \mu\text{m}$ 。详细仪器条件和数据获取详见 Hu 等(2012)。为了校正 ^{176}Lu 和 ^{176}Yb 对 ^{176}Hf 的干扰, 取 $^{176}\text{Lu}/^{175}\text{Hf}=0.026\,56$ 和 $^{176}\text{Yb}/^{173}\text{Yb}=0.793\,81$ (Blichert et al., 1997; Segal et al., 2003) 为定值。采用 $^{173}\text{Yb}/^{171}\text{Yb}=1.130\,17$ 和 $^{179}\text{Hf}/^{177}\text{Hf}=0.7325$ 分别对 Yb 同位素和 Hf 同位素进行指数归一化质量歧视校正 (Segal et al., 2003)。锆石标样 GJ-1 的 $^{176}\text{Hf}/^{177}\text{Hf}$ 标准值为 $0.282\,013 \pm 0.000\,019$ (Hu et al., 2012)。

3 错石 U-Pb 年龄及 Hf 同位素特征

3.1 铸石 U-Pb 年龄

东风岩体2件花岗岩样品DF01与DF02中的锆石均呈浅黄色至无色,绝大部分锆石晶型为自形-半自形;锆石为柱状,大小 $150\sim400\text{ }\mu\text{m}$,长轴与短轴之比多介于2~4,锆石的阴极发光图像均显示出岩浆锆石所特有的韵律环带(Hoskin et al., 2003; 吴元保等, 2004)(图4)。本次选择了环带清晰、无裂纹、锆石表面清晰的位置对其进行分析。

对样品 DF01 进行了共计 21 个点的测试(图 4, 表 1), 这些锆石的普通铅含量总体很低, 其中, 07、05 和 11 号测试点的年龄值明显高于其他测点, 对应

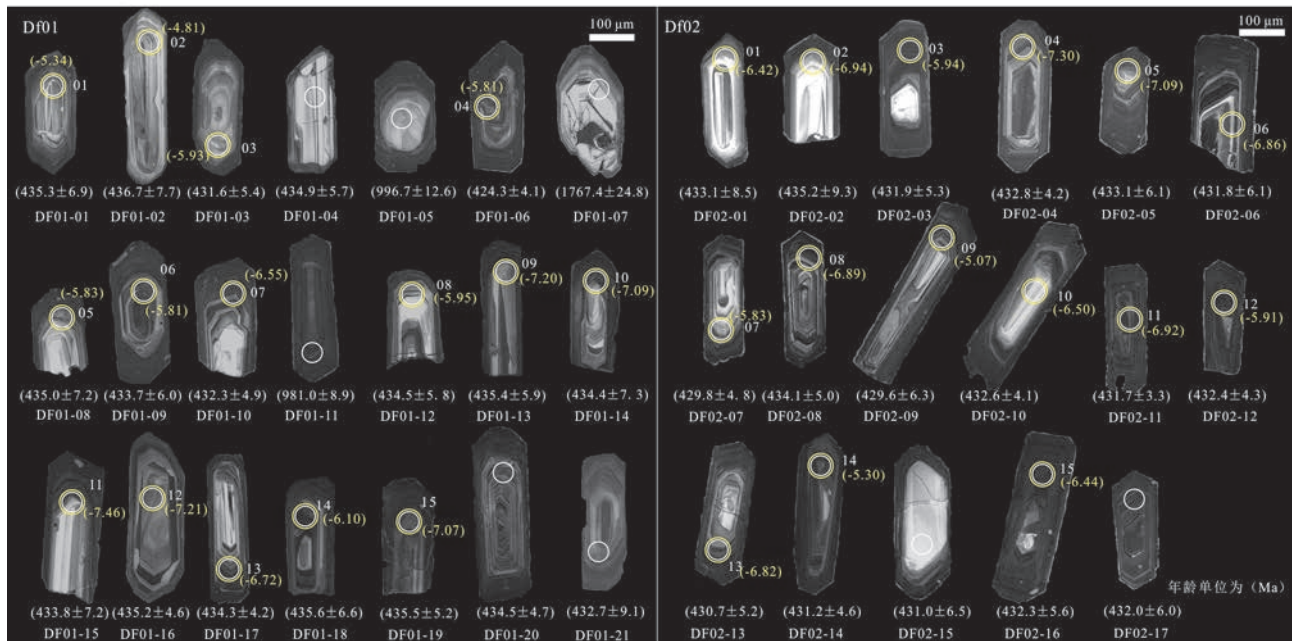


图4 东风花岗岩体的锆石阴极发光图像(白圈为U-Pb测试位置,黄圈为Hf同位素测试部位)

Fig. 4 CL images of zircon from the Dongfeng monzogranite (white and yellow circles indicating the laser spot of U-Pb dating and Hf isotope analysis, respectively)

的 $^{206}\text{Pb}/^{238}\text{U}$ 年龄值分别为 (1767.4 ± 24.8) Ma、 (996.7 ± 12.6) Ma、 (981.0 ± 8.9) Ma, 这些年龄值明显偏高的锆石为继承锆石。其余18个测点在U-Pb年龄曲线图(图5a)中的 $^{206}\text{Pb}/^{238}\text{U}$ 年龄值相接近, 其加权平均值为 (433.5 ± 2.6) Ma(MSWD=0.29)(图5b)。对样品DF02完成的17个点的分析测试(图4, 表1)结果表明, 锆石中的普通铅含量很低, 这17个点的 $^{206}\text{Pb}/^{238}\text{U}$ 年龄相近(图5c), 其加权平均值为 (432.0 ± 2.5) Ma(MSWD=0.06)(图5d)。

3.2 Hf同位素特征

对样品DF01和DF02锆石U-Pb测年的打点部位分别进行了15个点的Hf同位素测试(图4)。

本次分析的2件样品共计30颗锆石的 $^{176}\text{Yb}/^{177}\text{Hf}$ 和 $^{176}\text{Lu}/^{177}\text{Hf}$ 比值范围分别为0.007 212~0.041 416和0.000 234~0.001 628(表2), $^{176}\text{Lu}/^{177}\text{Hf}$ 比值均小于0.002, 表明这些锆石在形成以后, 仅具有较少放射成因Hf的积累, 因而可以用初始 $^{176}\text{Hf}/^{177}\text{Hf}$ 比值来代表锆石形成时的 $^{176}\text{Hf}/^{177}\text{Hf}$ 比值(吴福元等, 2007)。考虑到2件样品的 $f_{\text{Lu/Hf}}$ 的平均值为-0.97, 明显小于铁镁质地壳的 $f_{\text{Lu/Hf}}$ (-0.34, Ameilin et al., 1999)和硅铝质地壳的 $f_{\text{Lu/Hf}}$ (-0.72, Vervoort et al., 1996), 因此, 其二阶段模式年龄更能反映其源区物质从亏损

地幔抽取的时间(或其源区物质在地壳的平均存留年龄)。

其中, 样品DF01共15颗锆石的 $(^{176}\text{Hf}/^{177}\text{Hf})_i$ 的变化范围在0.282 300~0.282 374(表2, 图6b), Hf同位素成分比较均一, 加权平均值0.282 332, 对应的 $\varepsilon_{\text{Hf}}(t)$ 变化范围为-4.74~-7.45, 平均值-6.32(图6a,c); 地壳模式年龄(T_{DM2})变化范围1714~1882 Ma, 加权平均值1811 Ma(图6b)。

样品DF02共15颗锆石的 $(^{176}\text{Hf}/^{177}\text{Hf})_i$ 的变化范围0.282 305~0.282 369(表2, 图6b), Hf同位素成分比较均一, 加权平均值0.282 333, 对应的 $\varepsilon_{\text{Hf}}(t)$ 变化范围在-5.12~-7.28, 平均值-4.42(图6a,c), 地壳模式年龄(T_{DM2})变化范围1733~1871 Ma, 加权平均值1816 Ma(图6d)。

4 岩石地球化学特征

东风花岗岩体的主、微量元素分析结果见表3, 结果显示花岗岩 $w(\text{SiO}_2)$ 为68.48%~73.39%, 平均70.34, 稍低于中国花岗岩的平均含量(71.63%)(黎彤等, 1998), 从TAS图(图7a)可以看出, 所有点均落入花岗岩与花岗闪长岩区域; $w(\text{Al}_2\text{O}_3)$ 较高, 变化于

表 1 东风岩体花岗岩 LA-ICP-MS 的锆石 U-Pb 分析结果

Table 1 Zircon U-Pb dating results of the Dongfeng granitic pluton

样品点号	$w(B)/10^{-6}$	同位素比值						年龄/Ma							
		^{232}Th	^{238}U	Th/U	$^{207}\text{Pb}/^{206}\text{Pb}$	$\pm 1\sigma$	$^{207}\text{Pb}/^{235}\text{U}$	$\pm 1\sigma$	$^{206}\text{Pb}/^{238}\text{U}$	$\pm 1\sigma$	$^{207}\text{Pb}/^{206}\text{Pb}$	$\pm 1\sigma$	$^{207}\text{Pb}/^{235}\text{U}$	$\pm 1\sigma$	$^{206}\text{Pb}/^{238}\text{U}$
DF01-01	81	183	0.44	0.05447	0.00184	0.52602	0.01929	0.06986	0.00115	390.8	71.3	429.2	12.8	435.3	6.9
DF01-02	93	197	0.47	0.05456	0.00123	0.52645	0.01412	0.07008	0.00128	394.5	50.0	429.5	9.4	436.7	7.7
DF01-03	64	123	0.51	0.05394	0.00139	0.50964	0.01218	0.06924	0.00090	368.6	62.0	418.2	8.2	431.6	5.4
DF01-04	136	147	0.92	0.05316	0.00149	0.50856	0.01323	0.06979	0.00095	344.5	32.4	417.5	8.9	434.9	5.7
DF01-05	65	121	0.54	0.06619	0.00136	1.52293	0.03473	0.16720	0.00228	813.0	42.6	939.7	14.0	996.7	12.6
DF01-06	240	857	0.28	0.05080	0.00088	0.47728	0.00902	0.06804	0.00069	231.6	71.3	396.2	6.2	424.3	4.1
DF01-07	41	67	0.61	0.15644	0.00265	6.79408	0.14291	0.31543	0.00505	2417.6	28.7	2085	18.6	1767.4	24.8
DF01-08	95	141	0.67	0.05083	0.00198	0.48925	0.02044	0.06980	0.00119	231.6	90.7	404.4	13.9	435.0	7.2
DF01-09	229	939	0.24	0.04822	0.00090	0.45978	0.00897	0.06959	0.00099	109.4	44.4	384.1	6.2	433.7	6.0
DF01-10	172	575	0.30	0.04854	0.00090	0.46535	0.00969	0.06935	0.00082	124.2	42.6	388.0	6.7	432.3	4.9
DF01-11	188	432	0.43	0.06051	0.00106	1.37727	0.02644	0.16436	0.00160	620.4	37.8	879.3	11.3	981.0	8.9
DF01-12	67	135	0.49	0.04964	0.00206	0.47613	0.01956	0.06973	0.00096	189.0	96.3	395.4	13.5	434.5	5.8
DF01-13	137	463	0.30	0.04915	0.00122	0.47390	0.01284	0.06987	0.00097	153.8	59.3	393.9	8.8	435.4	5.9
DF01-14	109	453	0.24	0.05223	0.00133	0.50371	0.01450	0.06971	0.00121	294.5	59.3	414.2	9.8	434.4	7.3
DF01-15	63	136	0.46	0.05134	0.00195	0.49553	0.02045	0.06962	0.00120	257.5	88.9	408.7	13.9	433.8	7.2
DF01-16	79	304	0.26	0.05028	0.00127	0.48593	0.01255	0.06984	0.00077	209.3	57.4	402.1	8.6	435.2	4.6
DF01-17	141	277	0.51	0.05207	0.00136	0.50188	0.01297	0.06970	0.00070	287.1	59.3	413.0	8.8	434.3	4.2
DF01-18	143	434	0.33	0.05269	0.00138	0.51205	0.01575	0.06991	0.00110	322.3	59.3	419.8	10.6	435.6	6.6
DF01-19	115	376	0.30	0.05447	0.00121	0.52477	0.01174	0.06990	0.00086	390.8	50.0	428.3	7.8	435.5	5.2
DF01-20	175	430	0.41	0.05585	0.00119	0.54087	0.01251	0.06972	0.00078	455.6	48.1	439.0	8.2	434.5	4.7
DF01-21	93	279	0.33	0.05697	0.00164	0.55239	0.01754	0.07007	0.00114	494.5	51.8	438.8	9.3	432.7	9.1
DF02-01	19	94	0.60	0.05710	0.00136	0.54054	0.01411	0.06943	0.00150	427.8	57.4	431.3	9.9	433.1	8.5
DF02-02	16	68	0.50	0.05535	0.00144	0.52923	0.01496	0.06949	0.00141	509.3	31.5	447.2	7.8	435.2	9.3
DF02-03	109	291	0.24	0.05746	0.00083	0.55344	0.01191	0.06984	0.00155	387.1	42.6	427.0	7.2	431.9	5.3
DF02-04	25	95	0.39	0.05439	0.00102	0.52273	0.01085	0.06930	0.00088	344.5	37.0	419.4	5.6	432.8	4.2
DF02-05	49	159	0.30	0.05316	0.00088	0.51143	0.00841	0.06944	0.00069	405.6	38.9	430.3	6.9	433.1	6.1
DF02-06	51	158	0.29	0.05481	0.00094	0.52770	0.01032	0.06949	0.00101	298.2	48.1	410.9	7.4	431.8	6.1
DF02-07	24	92	0.40	0.05228	0.00109	0.49875	0.01096	0.06928	0.00101	376.0	77.8	422.3	12.1	429.8	4.8
DF02-08	33	115	0.34	0.05413	0.00186	0.51569	0.01808	0.06894	0.00080	316.7	35.2	417.7	6.2	434.1	5.0
DF02-09	65	188	0.26	0.05269	0.00084	0.50891	0.00926	0.06966	0.00082	435.2	134.2	432.3	16.8	429.6	6.3
DF02-10	48	259	0.68	0.05560	0.00252	0.53067	0.02528	0.06891	0.00105	542.6	33.3	452.2	5.9	432.6	4.1
DF02-11	79	211	0.26	0.05834	0.00085	0.56102	0.00906	0.06940	0.00067	588.9	29.6	457.5	5.4	431.7	3.3
DF02-12	123	277	0.20	0.05934	0.00082	0.56926	0.00836	0.06926	0.00055	388.9	37.0	424.9	6.1	432.4	4.3
DF02-13	32	102	0.30	0.05423	0.00088	0.51970	0.00913	0.06938	0.00072	390.8	61.1	423.2	9.7	430.7	5.2
DF02-14	16	83	0.60	0.05447	0.00147	0.51704	0.01455	0.06910	0.00086	416.7	54.6	428.1	9.0	431.2	4.6
DF02-15	19	97	0.68	0.05515	0.00144	0.52449	0.01352	0.06918	0.00077	388.9	40.7	425.0	8.1	431.0	6.5
DF02-16	59	182	0.27	0.05423	0.00097	0.51973	0.01211	0.06915	0.00107	300.1	48.1	410.5	7.4	432.3	5.6
DF02-17	31	102	0.31	0.05215	0.00108	0.49821	0.01096	0.06936	0.00093	300.0	48.0	410.0	7.0	432.0	6.0

12.82%~15.09%，平均 14.15%，A/CNK 值为 1.12~1.43，A/NK 值 1.42~1.88，在 A/CNK-A/NK 图解(图 7b)中，均落入过铝质区域； $w(\text{K}_2\text{O} + \text{Na}_2\text{O})$ 为 5.94%~8.42%，平均 7.03%； $\text{K}_2\text{O}/\text{Na}_2\text{O}$ 值变化于 1.26~2.36，平均 1.79，表现为富 K 的特征；在 $\text{K}_2\text{O}-\text{SiO}_2$ 图解(图

7c) 中，样品均落在高钾钙碱性系列与钾玄岩系列。

东风岩体花岗岩具有与万洋山岩体、彭公庙岩体二长花岗岩相同的微量元素和稀土元素基本一致的特征(图 8)。东风岩体花岗岩的稀土元素总体含量中等(表 3)， ΣREE 为 $(140\text{--}186)\times 10^{-6}$ ， $\Sigma \text{LREE}/$

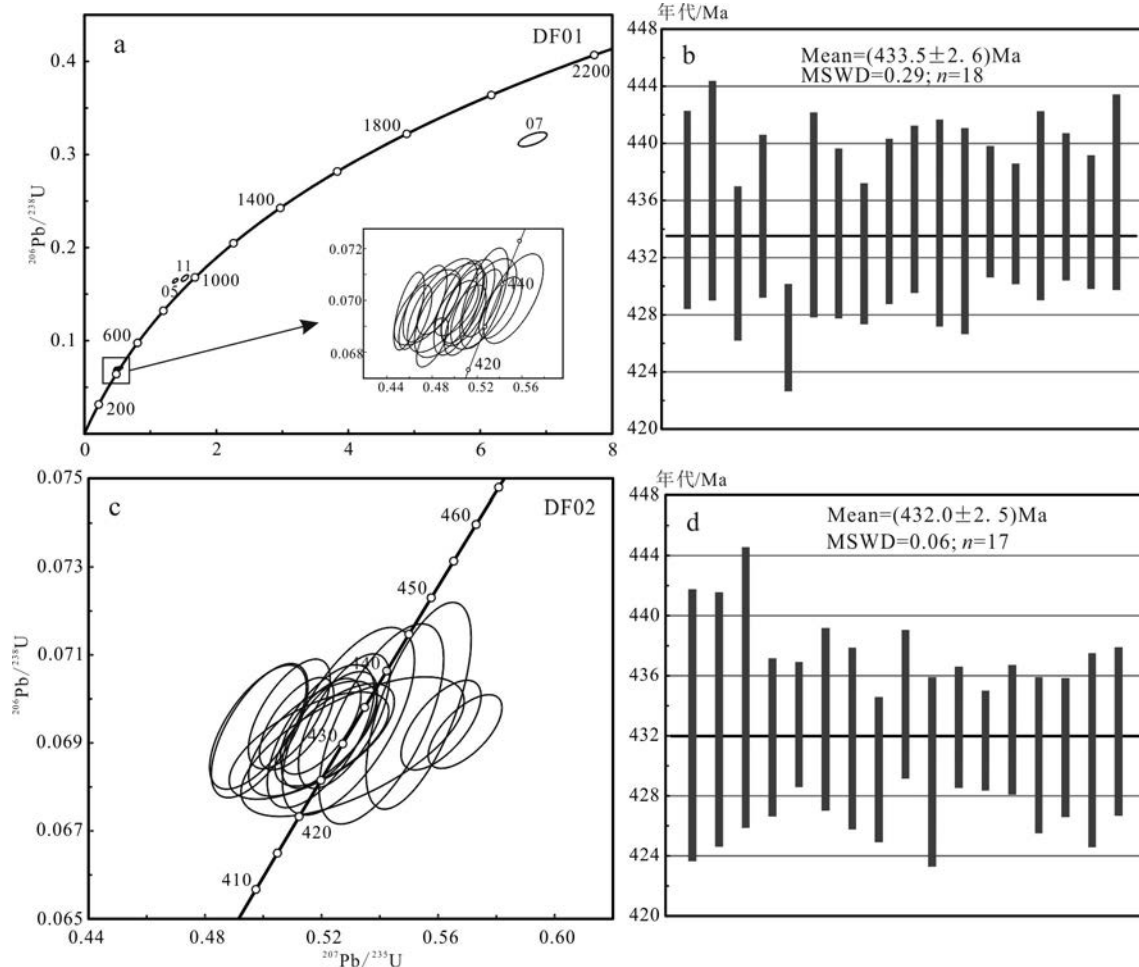


图 5 东风花岗岩体的锆石 U-Pb 谱和曲线图(a,c)和加权平均年龄图(b,d)

Fig. 5 LA-ICPMS U-Pb Concordia age plots (a, c) and weighted average diagrams for zircons (b, d) from the Dongfeng monzogranite

Σ HREE 值为 1.72~2.22, 表明东风岩体花岗岩轻、重稀土元素分馏较明显, δ Eu 值为 0.41~0.75, 平均值 0.56。在稀土元素配分模式图(图 8a)中, 东风岩体花岗岩显示为一明显右倾的曲线, 配分曲线具有较明显的 Eu 负异常, 同时, LREE 一侧相对较陡(分馏明显)、重稀土元素部分较为平坦(分馏不明显)的特征。HREE 的相对亏损可能与锆石、磷灰石、独居石等的分离结晶有关, 而 Eu 负异常明显则反映出岩浆结晶作用过程中斜长石、钾长石的分离结晶作用较明显。相较于花岗岩基岩, 风化层花岗岩稀土矿体(湖南省核工业地质局 301 队, 2018)中的稀土元素(除 Ce 外)均有明显富集, 尤其是重稀土元素富集更加明显(图 8b), Eu 负异常也更加明显, 配分曲线整体相对较平坦。

从以原始地幔对岩体微量元素进行标准化的微量元素蛛网图(图 8c)中可以看出, 东风岩体花岗岩

不相容元素 Rb、(Th+U)、Nd、(Zr+Hf)富集, 而 Ba、Nb、Sr、P、Ti 明显亏损, 显示出壳源花岗岩的特征 (Chappell et al., 1992; Bea et al., 2011; Dong et al., 2013)。微量元素 Ba、Sr 亏损, 说明岩石中存在有斜长石的熔融残留相或结晶分离相(Patino et al. 1991; 1995), P、Ti 亏损可能与磷灰石、钛铁矿的分离结晶有关, 而 Nb 可能由于富集到含钛的黑云母中而出现亏损(李昌年, 1992), 同时, Nb、Ta 发生了较明显分馏, 显示 Nb 相对亏损而 Ta 相对富集, 也暗示花岗岩具有壳源花岗岩特征(陈小明等, 2002)。

5 讨 论

5.1 东风岩体的侵位年龄

以往关于东风岩体的研究较少, 仅在湖南省地质调查院(1972; 2005)完成的 1:20 万永兴幅区域地

表2 东风花岗岩体的锆石Hf同位素组成

Table 2 Zircon Hf isotopic data of the Dongfeng granitic pluton

样品点号	年龄/Ma	$^{176}\text{Yb}/^{177}\text{Hf}$	$^{176}\text{Lu}/^{177}\text{Hf}$	$^{176}\text{Hf}/^{177}\text{Hf}$	2σ	$\varepsilon_{\text{Hf}}(0)$	$\varepsilon_{\text{Hf}}(t)$	T_{DM1}/Ma	T_{DM2}/Ma	$f_{\text{Lu/Hf}}$
DF01-01	435.3	0.024900	0.001015	0.282360	0.000016	-14.58	-5.30	1261	1748	-0.97
DF01-02	436.7	0.023967	0.000942	0.282374	0.000014	-14.08	-4.74	1238	1714	-0.97
DF01-03	431.6	0.023993	0.000972	0.282343	0.000016	-15.19	-5.97	1283	1788	-0.97
DF01-04	424.3	0.023736	0.000958	0.282346	0.000019	-15.07	-6.01	1278	1784	-0.97
DF01-05	435.0	0.021173	0.000863	0.282345	0.000019	-15.11	-5.79	1277	1779	-0.97
DF01-06	433.7	0.025003	0.000987	0.282346	0.000025	-15.06	-5.81	1279	1779	-0.97
DF01-07	432.3	0.029973	0.001036	0.282326	0.000030	-15.78	-6.57	1309	1826	-0.97
DF01-08	434.5	0.028634	0.001081	0.282343	0.000039	-15.17	-5.93	1286	1787	-0.97
DF01-09	435.4	0.037054	0.001417	0.282310	0.000038	-16.32	-7.16	1344	1865	-0.96
DF01-10	434.4	0.038118	0.001556	0.282314	0.000018	-16.18	-7.07	1343	1859	-0.95
DF01-11	433.8	0.027766	0.001031	0.282300	0.000025	-16.70	-7.45	1345	1882	-0.97
DF01-12	435.2	0.007212	0.000234	0.282301	0.000018	-16.67	-7.17	1316	1866	-0.99
DF01-13	434.3	0.034256	0.001364	0.282323	0.000024	-15.86	-6.70	1323	1836	-0.96
DF01-14	435.6	0.024174	0.000968	0.282338	0.000023	-15.35	-6.05	1290	1796	-0.97
DF01-15	435.5	0.025263	0.001001	0.282311	0.000021	-16.31	-7.02	1329	1857	-0.97
DF02-01	433.1	0.028238	0.001108	0.282331	0.000025	-15.60	-6.40	1304	1815	-0.97
DF02-02	435.2	0.028170	0.001098	0.282316	0.000018	-16.12	-6.87	1324	1847	-0.97
DF02-03	431.9	0.041416	0.001648	0.282349	0.000013	-14.97	-5.94	1298	1786	-0.95
DF02-04	432.8	0.026685	0.001039	0.282305	0.000025	-16.50	-7.28	1337	1871	-0.97
DF02-05	433.1	0.019290	0.000650	0.282308	0.000015	-16.41	-7.07	1320	1858	-0.98
DF02-06	431.8	0.028671	0.001122	0.282318	0.000016	-16.04	-6.86	1322	1844	-0.97
DF02-07	429.8	0.028706	0.001119	0.282347	0.000025	-15.01	-5.88	1281	1780	-0.97
DF02-08	434.1	0.010141	0.000343	0.282311	0.000015	-16.29	-6.85	1305	1845	-0.99
DF02-09	429.6	0.027864	0.001092	0.282369	0.000013	-14.26	-5.12	1251	1733	-0.97
DF02-10	432.6	0.029583	0.001157	0.282329	0.000032	-15.67	-6.49	1309	1821	-0.97
DF02-11	431.7	0.027559	0.001115	0.282317	0.000020	-16.10	-6.93	1324	1848	-0.97
DF02-12	432.4	0.019608	0.000781	0.282343	0.000017	-15.19	-5.90	1277	1784	-0.98
DF02-13	430.7	0.021711	0.000836	0.282317	0.000075	-16.08	-6.85	1314	1842	-0.97
DF02-14	431.2	0.037607	0.001520	0.282366	0.000029	-14.37	-5.32	1269	1746	-0.95
DF02-15	432.3	0.023397	0.000918	0.282329	0.000018	-15.68	-6.44	1301	1818	-0.97

注: $\varepsilon_{\text{Hf}}(t)=10000 \times \{[(^{176}\text{Hf}/^{177}\text{Hf})_s - (^{176}\text{Lu}/^{177}\text{Hf})_s \times (e^{(\lambda t)} - 1)] / [(^{176}\text{Hf}/^{177}\text{Hf})_{\text{CHUR},0} - (^{176}\text{Lu}/^{177}\text{Hf})_{\text{CHUR}} \times (e^{(\lambda t)} - 1)] - 1\}$; $T_{\text{DM1}}=1/\lambda \times \ln\{1 + [(^{176}\text{Hf}/^{177}\text{Hf})_s - (^{176}\text{Hf}/^{177}\text{Hf})_{\text{DM}}] / [(^{176}\text{Hf}/^{177}\text{Hf})_s - (^{176}\text{Hf}/^{177}\text{Hf})_{\text{DM}}]\}$; $T_{\text{DM2}}=T_{\text{DM1}} - (T_{\text{DM1}} - t) \times [f_{\text{cc}} - f_s] / (f_{\text{cc}} - f_{\text{DM}})$; $f_{\text{Lu/Hf}}=(^{176}\text{Lu}/^{177}\text{Hf})_s / (^{176}\text{Lu}/^{177}\text{Hf})_{\text{CHUR}} - 1$, 其中, $\lambda=1.867 \times 10^{-11}/\text{a}$ (Soderlund et al., 2004); $(^{176}\text{Lu}/^{177}\text{Hf})_s$ 和 $(^{176}\text{Hf}/^{177}\text{Hf})_s$ 为样品同位素组成; $(^{176}\text{Lu}/^{177}\text{Hf})_{\text{CHUR}}=0.0332$ and $(^{176}\text{Hf}/^{177}\text{Hf})_{\text{CHUR},0}=0.282772$ (Blichert-Toft et al., 1997); $(^{176}\text{Lu}/^{177}\text{Hf})_{\text{DM}}=0.0384$, $(^{176}\text{Hf}/^{177}\text{Hf})_{\text{DM}}=0.28325$ (Griffin et al., 2000); $(^{176}\text{Lu}/^{177}\text{Hf})_{\text{mean crust}}=0.015$; $f_{\text{cc}}=[(^{176}\text{Lu}/^{177}\text{Hf})_{\text{mean crust}} / (^{176}\text{Lu}/^{177}\text{Hf})_{\text{CHUR}}]-1$; $f_s=f_{\text{Lu/Hf}}$; $f_{\text{DM}}=[(^{176}\text{Lu}/^{177}\text{Hf})_{\text{DM}} / (^{176}\text{Lu}/^{177}\text{Hf})_{\text{CHUR}}]-1$; t =锆石结晶年龄。

质矿产调查与1:25万衡阳幅区域地质矿产调查报告中提到将其形成年龄定为加里东期,但并未有准确的年代学数据作为支撑。

本次对东风岩体采集的2件粗中粒黑云母二长花岗岩锆石样品(DF01、DF02)的LA-ICP-MS U-Pb定年结果分别为(433.5 ± 2.6)Ma和(432.0 ± 2.5)Ma,两者在误差范围内非常一致,可以代表东风岩体的形成年龄。同时,2件样品的年龄与沈渭洲等(2008)利用LA-ICP-MS U-Pb定年获得的万洋山岩体黑云

母二长花岗岩形成年龄(433.8 ± 2.2)Ma一致,与张文兰等(2011)获得彭公庙岩体两件中粗粒黑云母花岗岩锆石LA-ICP-MS U-Pb的定年结果(435.3 ± 2.7)Ma和(436.2 ± 3.1)Ma在误差范围内也相同。东风岩体侵位年龄433 Ma左右,根据前人对华南加里东花岗岩早晚期岩浆活动的侵位时限划分标准(舒良树,2006;张芳荣等,2009),东风岩体的形成年龄对应于加里东晚期。这与野外所观察到岩体与奥陶系天马山组呈侵入接触关系、外接触带见有明显的角岩化

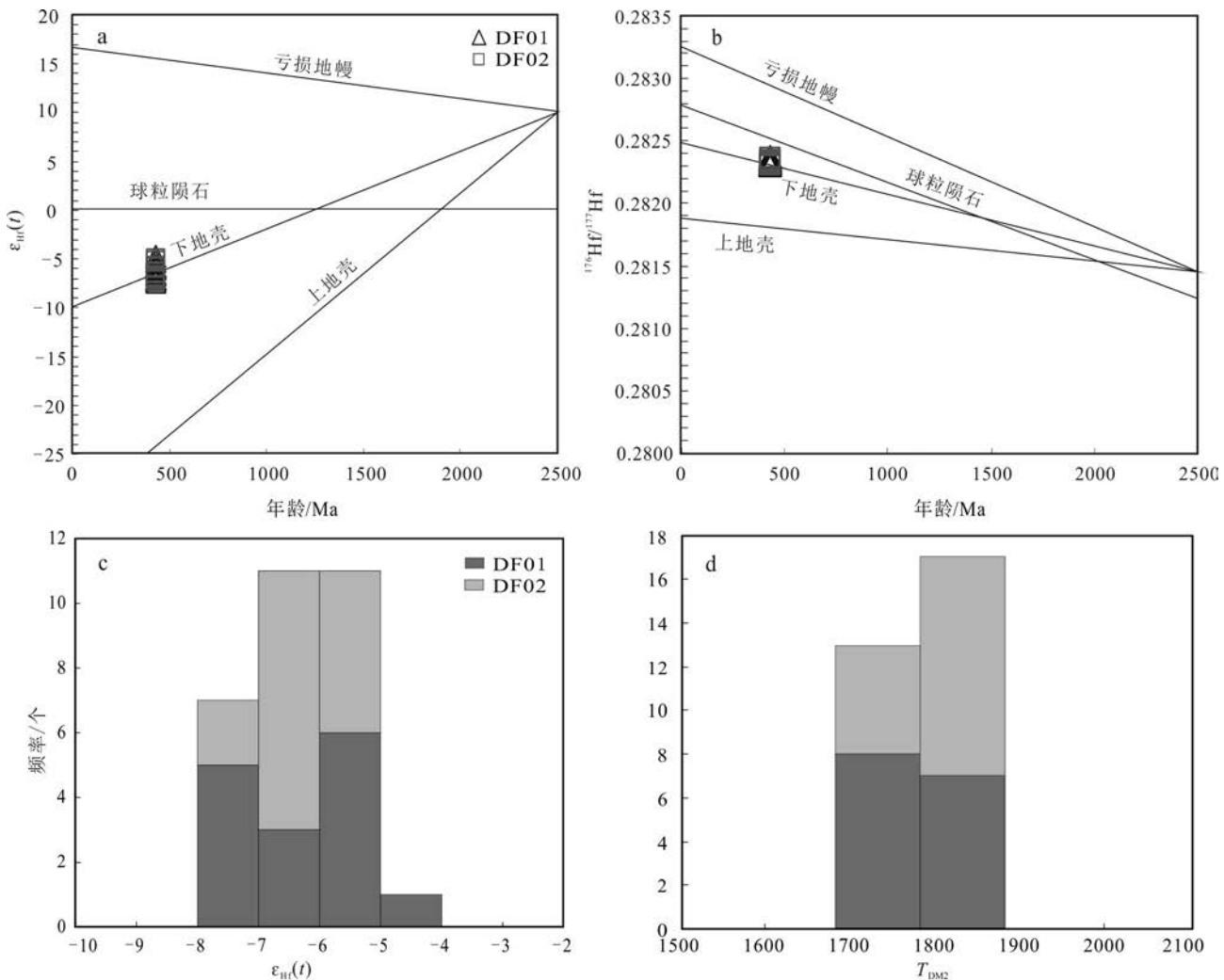


图6 东风岩体花岗岩锆石 $\epsilon_{\text{Hf}}(t)$ 值图解(a)、 $^{176}\text{Hf}/^{177}\text{Hf}$ 比值U-Pb年龄图解(b)、锆石 $\epsilon_{\text{Hf}}(t)$ 值图解(c)和Hf同位素地壳模式年龄(T_{DM2})柱状图(d)

Fig. 6 $\epsilon_{\text{Hf}}(t)$ ages diagram(a), $^{176}\text{Hf}/^{177}\text{Hf}$ U-Pb ages diagram(b), histogram of zircon $\epsilon_{\text{Hf}}(t)$ ages(c) and histogram of zircon Hf-isotope crust model age (T_{DM2})(d) of the Dongfeng granitic pluton

等蚀变的地质现象相符。此外,东风岩体花岗岩与彭公庙岩体、万洋山岩体二长花岗岩具有相同的微量元素特征(图8),暗示这3个岩体的加里东期花岗岩有可能为起源于同一岩浆房的岩浆同时侵位形成,岩体在深部有可能相连。

5.2 岩体的成因类型及地质背景

东风花岗岩体黑云母二长花岗岩具有高钾钙碱性、强过铝质特征(图7b、c),铝饱和指数A/CNK值均大于1.1(1.12~1.43),经过标准矿物计算得到的刚玉分子含量为1.87%~4.82%; $^{10}\text{Ga}/\text{Al}$ 值介于2.13~2.64,平均值(2.44)小于A型花岗岩的最低值(2.6)(Whalen et al., 1987),在岩石类型判别图解(图9a)中,测点均落入I&S型花岗岩区域

或附近,在 $w(\text{K}_2\text{O})-w(\text{Na}_2\text{O})$ 图解(图9b)中,样品落点较分散,但除个别点落入A型花岗岩区域内,大多数的点均落入S型花岗岩区域内或附近,这些特征均表明东风岩体花岗岩的岩石类型为S型花岗岩。

在稀土元素配分图(图8a)中,东风岩体花岗岩稀土元素显示一条明显右倾的曲线,其轻、重稀土元素比值LREE/HREE较高(5.32~6.86)。岩体具有较高的Yb含量、大离子亲石元素(LILE)含量以及相对较低的HREE、Sr和高场强元素(HFSE)含量,以及计算得到的分异系数(Di)为80.38~86.95(表3),这些特征均显示东风岩体花岗岩岩浆可能经历了一定程度的结晶分异作用,但其Nb/Ta值介于6.56~10.90(平均9.26),Zr/Hf值介于34.49~38.45(平均35.04),

表 3 东风岩体花岗岩样品的主量元素($w(\text{B})/\%$)和微量元素($w(\text{B})/10^{-6}$)分析结果Table 3 Major and trace element compositions of the Dongfeng granitic pluton ($w(\text{B})/\%$) and trace elements

$w(\text{B})/10^{-6}$													
组分	MT01	MT02	MT03	MT04	MT05	MT06	组分	MT01	MT02	MT03	MT04	MT05	MT06
SiO_2	68.48	71.42	73.39	70.18	69.64	68.91	Ce	75.9	77	56.4	69.2	79	54.6
TiO_2	0.55	0.48	0.34	0.43	0.52	0.45	Pr	8.55	7.5	6.87	7.08	10.4	6.45
Al_2O_3	14.93	13.01	12.82	14.35	14.71	15.09	Nd	33.3	29.2	26.2	26.0	39.2	24.9
TFe_2O_3	4.63	4.19	3.03	3.84	4.41	3.82	Sm	7.50	6.71	5.76	6.26	8.17	5.66
MnO	0.11	0.11	0.08	0.11	0.10	0.10	Eu	1.34	0.95	1.09	1.15	1.38	1.41
MgO	1.00	1.12	0.69	0.85	1.05	0.90	Gd	7.32	7.53	5.72	6.28	7.97	5.76
CaO	1.48	1.60	1.13	2.00	1.34	1.57	Tb	1.12	1.19	0.886	1.07	1.16	0.908
Na_2O	2.45	2.48	2.13	3.06	2.47	2.70	Dy	6.97	7.42	5.16	6.26	7.17	5.12
K_2O	5.19	3.62	5.02	3.86	3.47	5.72	Ho	1.37	1.55	0.96	1.20	1.30	1.01
P_2O_5	0.16	0.12	0.09	0.10	0.14	0.11	Er	3.95	4.8	3.11	3.67	3.96	3.17
SO_3	0.02	0.01	0.01	0.01	0.01	0.02	Tm	0.55	0.66	0.47	0.52	0.53	0.44
SrO	0.02	0.02	0.01	0.01	0.02	0.01	Yb	4.02	4.74	3.23	3.83	3.81	2.81
烧失量	1.26	1.46	0.85	0.84	1.85	0.61	Lu	0.53	0.68	0.43	0.51	0.48	0.39
总和	100.28	99.64	99.59	99.64	99.73	100.01	Hf	4.76	6.06	4.36	4.81	6.08	5.27
$\text{K}_2\text{O}+\text{Na}_2\text{O}$	7.64	6.10	7.15	6.92	5.94	8.42	Ta	1.33	1.41	0.91	1.82	1.57	0.95
$\text{K}_2\text{O}/\text{Na}_2\text{O}$	2.12	1.46	2.36	1.26	1.40	2.12	W	1.43	2.31	9.83	4.9	2.98	4.95
A/NCK	1.21	1.19	1.16	1.12	1.43	1.12	Pb	41.88	33.82	40.12	33.71	29.51	41.66
A/NK	1.55	1.62	1.43	1.56	1.88	1.42	Th	18.5	17.9	15.3	17.8	21.6	12.9
σ	2.27	1.3	1.67	1.75	1.31	2.72	U	3.60	4.68	2.71	3.48	4.24	3.95
Di	81.87	81.58	86.95	81.56	80.38	83.72	$^{10^4}\text{Ga}/\text{Al}$	2.56	2.64	2.17	2.63	2.54	2.13
V	55.3	53.1	39.1	48.8	55.2	50	Zr/Hf	38.45	34.49	34.86	32.64	34.70	35.10
Cr	29.1	48.3	26.6	41.2	27.7	29.9	Nb/Ta	10.71	9.40	9.53	6.56	8.48	10.90
Ga	20.2	18.2	14.7	20	19.8	17	Th/U	5.14	3.82	5.65	5.11	5.09	3.27
Rb	212	177	188	236	171	212	ΣREE	241.61	233.63	184.17	210.53	262.43	189.63
Sr	101	105	89.1	90.5	99.1	128	LREE	160.49	151.96	125.12	138.39	180.85	120.02
Y	55.3	53.1	39.1	48.8	55.2	50.0	HREE	81.13	81.68	59.05	72.14	81.58	69.61
Zr	183	209	152	157	211	185	L/H	1.98	1.86	2.12	1.92	2.22	1.72
Nb	14.21	13.22	8.70	11.95	13.29	10.39	(La/Yb) _N	6.05	4.63	6.40	5.38	8.04	6.89
Sn	6.98	6.35	5.22	14.00	3.22	4.98	Y/ ΣREE	0.23	0.23	0.21	0.23	0.21	0.26
Cs	11.80	11.30	8.52	30.50	11.50	8.27	δEu	0.54	0.41	0.57	0.55	0.52	0.75
Ba	731	455	719	298	438	917	δCe	1.06	1.21	0.95	1.16	0.89	0.98
La	33.9	30.6	28.8	28.7	42.7	27.0	TZr/°C	808.8	824.9	795.7	789.5	840.3	801.5

注:比值单位为 1。

显示其远没有达到高分异花岗岩($\text{Nb}/\text{Ta} < 5$, $\text{Zr}/\text{Hf} < 26$, Bau, 1996; Ballouard et al., 2016; 吴福元等, 2017)的程度。

从微量元素进行标准化的微量元素蛛网图(图 8c)可以看出, 样品均具有明显的 Rb、(Th+U)、Nd、($\text{Zr}+\text{Hf}$)富集, 而 Ba、Nb、Sr、P、Ti 亏损, 表明东风岩体花岗岩具有地壳物质熔融产物的特征(Chappell et al., 1992; 凤永刚等, 2008; Bea et al., 2011; Dong et al., 2013)。

Hf 同位素示踪研究已经广泛地应用于一些重要

地球化学储库(如亏损地幔、球粒陨石和地壳等)的源区判别(吴福元等, 2007)。东风岩体两件花岗岩样品单颗粒锆石的 Hf 同位素组成都比较均一, 具有相似的 $\varepsilon_{\text{Hf}}(t)$ 值变化范围(集中于 -11~ -5, 表 2, 图 6c), 且 Hf 同位素二阶段模式年龄非常集中(变化于 1.71~1.88 Ga, 表 3, 图 6d)。Hf 同位素 $\varepsilon_{\text{Hf}}(t) < 0$ 表明岩石为古老地壳部分熔融而形成(Vervoort et al., 1996; Griffin et al., 2002; 2006), 东风岩体花岗岩 $\varepsilon_{\text{Hf}}(t) < 0$, 且在 $\varepsilon_{\text{Hf}}(t)$ - t 图解(图 6a)和 $^{176}\text{Hf}/^{177}\text{Hf}$ - t 图解(图 6b)中, 样品点均集中分布于亏损地幔线及球粒

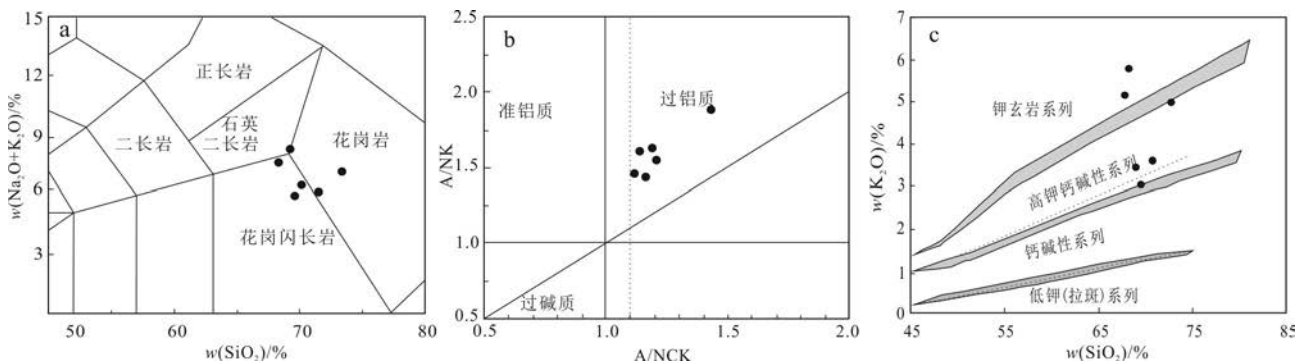


图7 东风岩体花岗岩TAS图解(a, 底图据Le Bas, 1986)、ANK-ACNK图解(b, 底图据Rollinson, 1993)和 $w(K_2O)$ - $w(SiO_2)$ 图解(c, 底图据Maniar et al., 1989)

Fig. 7 TAS diagram (a, base map after Le Bas et al., 1986), ANK-ACNK diagram (b, base map after Rollinson, 1993) and $w(K_2O)$ - $w(SiO_2)$ diagram (c, base map after Maniar et al., 1989) of the Dongfeng monzogranite

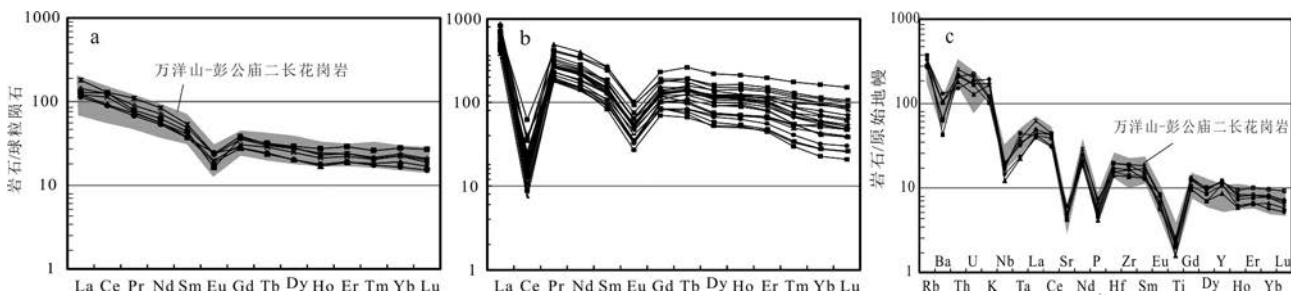


图8 东风岩体花岗岩基岩(a)、风化层(b)稀土元素球粒陨石标准化图和东风岩体花岗岩基岩微量元素原始地幔标准化蛛网图(c)(标准化值据Boynton, 1984; Sun et al., 1989)

万洋山岩体、彭公庙岩体二长花岗岩数据来源自柏道远等, 2006; 伍光英等, 2008; 陈迪等, 2016; 风化层数据源自湖南省核工业地质局301队, 2018

Fig. 8 Chondrite-normalized REE patterns for the Dongfeng monzogranite (a) and REE ore body (b), and primitive mantle-normalized trace element spider diagram for the Dongfeng monzogranite (c) (chondrite and mantle values after Boynton, 1984; Sun et al., 1989) Wanyangshan and Penggongmiao data are from Bai et al., 2006; Wu et al., 2008; Chen et al., 2016; REE values in Ore body from 301 Brigade of Hunan Nuclear Geological Bureau, 2018

陨石演化线之下(Wu et al., 2006; 吴福元等, 2007), 由此可推断东风岩体花岗岩为古老地壳物质部分熔融的产物。二阶段模式年龄介于1714~1882 Ma, 样品DF01的继承锆石(点07)的形成年龄也在此范围内, 与前人统计得到的华夏板块Hf同位素二阶段模式年龄(Xu et al., 2007; Yu et al., 2010; Zhao et al., 2013)一致, 而明显区别于扬子地块(Liu et al., 2008; Zhao et al., 2013)。

综上所述, 东风岩体的微量元素特征、锆石Hf同位素特征以及继承锆石的形成年龄均表明东风岩体成岩物质来源于华夏地块古老地壳物质的部分熔融。尽管岩浆结晶锆石没有显著幔源特征的Hf同位素记录, 但是计算显示东风岩体花岗岩具有较高

的“锆石饱和温度”(Watson et al., 1983)(789.5~824.9°C, 平均810°C, 表3), 暗示地幔岩浆很可能为花岗岩的形成提供了热源(王涛等, 2013; 任飞等, 2021)。

前人对华南地区加里东期构造环境的研究表明, 460~440 Ma期间扬子地块和华夏地块发生陆内俯冲和汇聚挤压, 造山带发生快速褶皱缩短和逆冲加厚(舒良树等, 2008)而形成岩石圈山根。其后岩石圈地幔与软流圈之间对流, 引起岩石圈拆沉和上地幔的隆起, 导致幔源岩浆的产生和底侵, 引起下地壳的部分熔融, 同时后碰撞构造环境下深大断裂(本区为茶陵—郴州大断裂, 图1a)伸展松弛促使中下地壳减压熔融, 从而诱发了南岭在440~420 Ma期间的

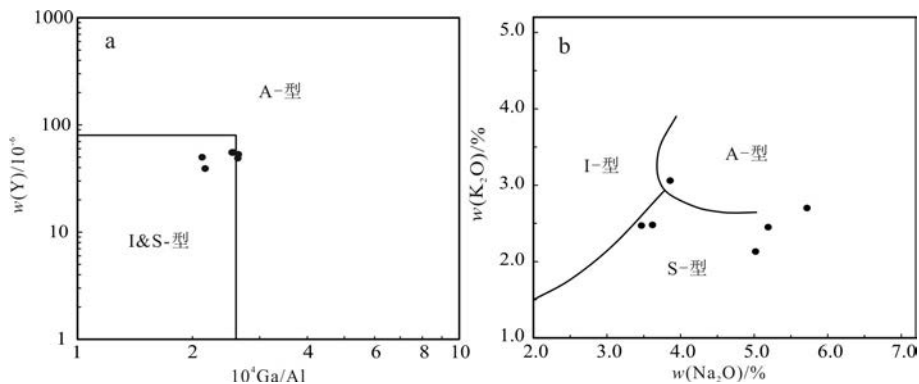


图9 东风岩体花岗岩的 $w(Y)$ -Ga/Al图解(a,底图据Whalen et al., 1987)和 $w(K_2O)$ - $w(Na_2O)$ 图解(b,底图据Collins et al., 1982)的构造判别图解
Fig. 9 $w(Y)$ -Ga/Al diagram (a, base map after Whalen et al., 1987) and $w(K_2O)$ - $w(Na_2O)$ diagram (b, base map after Collins et al., 1982) of the Dongfeng monzogranite

大面积中酸性岩浆(本区为万洋山—彭公庙等岩体)的侵入活动(徐先兵等, 2009; Wang et al., 2007b; 2010; Wan et al., 2010; Li et al., 2010; 张菲菲等, 2010; 程顺波等, 2013; 2016; Chen et al., 2019)。

在微量元素构造判别图解(图10)中,东风岩体与邻区万洋山岩体、彭公庙岩体加里东期花岗岩一样,所有数据点均落入后碰撞区域(Post-CLOG),进一步表明东风岩体形成于后碰撞环境。

综上所述,东风岩体形成于扬子板块与华夏板块陆内汇聚后的后碰撞伸展环境,为增厚地壳减压熔融和软流圈地幔上涌诱发古老地壳物质发生重熔作用形成的S型花岗岩。

5.3 东风稀土矿床特征

近年来对南岭地区风化壳离子吸附型稀土矿的研究显示,加里东期(王彦斌等, 2010; 孙艳等, 2012; 赵芝等, 2012)、印支期(于扬等, 2012; 张爱梅等, 2010; 郑国栋等, 2012)和燕山期(陈正宏等, 2008; Li et al., 2003; 李建康等, 2012)的花岗岩均可作为稀土矿床的成矿母岩(王登红等, 2013; 赵芝等, 2014),因此,离子吸附型稀土矿床的形成对花岗岩的时代没有选择性。原岩中稀土元素的含量则对矿床的形成起到关键性的作用,花岗岩岩体原岩中稀土元素丰度愈高,对成矿愈有利,稀土矿床的母岩在成岩过程中一般经历过稀土元素的预富集过程(周美夫等, 2020)。南岭离子吸附型稀土元素矿体一般比基岩中的稀土元素含量富集2~5倍,因此,在基岩的稀土丰度大于 150×10^{-6} 的情况下就可形成离子吸附型稀土矿床(苏晓云等, 2014)。一般富轻稀土元素的花岗岩母岩经风化后形成轻稀土型风化壳,富重稀土

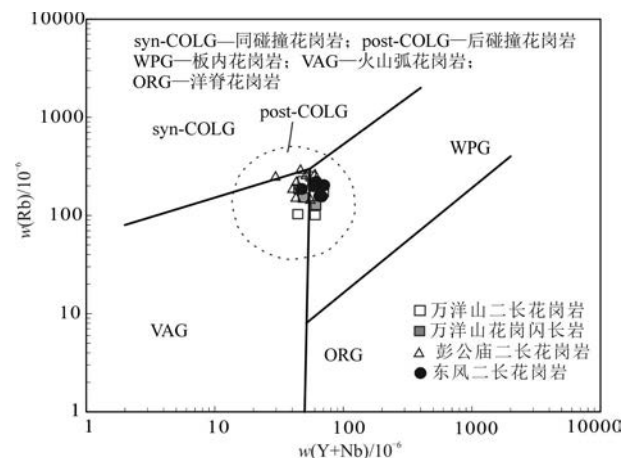


图10 东风岩体构造判别图解(底图据Pearce et al., 1984; 1996)
万洋山岩体、彭公庙岩体数据引自柏道远等, 2006; 伍光英等, 2008;
陈迪等, 2016

Fig. 10 Tectonic setting discrimination diagram of the Dongfeng pluton (base map after Pearce et al., 1984; 1996)
Wanyangshan and Penggongmiao data are from Bai et al., 2006; Wu et al., 2008; Chen et al., 2016

元素者则风化形成重稀土风化壳,但近年在赣南地区也有轻稀土矿床中有重稀土矿体的报道(王登红等, 2017; 陈斌锋等, 2019; 赵芝等, 2022)。

东风岩体花岗岩基岩中的稀土元素总量 Σ REE为 $(184.2\sim264.2) \times 10^{-6}$ (表3),要高于南岭地区已知的4个含稀土矿的徐敦、竹州、宁化、益将加里东期花岗岩体的稀土元素含量 $((124\sim224) \times 10^{-6}$,地矿部南岭项目组, 1989; 王彦斌等, 2010)。LREE/HREE值介于1.72~2.22,显示出轻稀土元素富集的特征,其中,岩体中的 $w(Y)$ 非常高,为 $(39.1\sim55.3) \times 10^{-6}$ (表

3), $Y/\Sigma REE=21\% \sim 26\%$, 属于高 Y 型花岗岩(张旗等, 2022), 因此, 东风稀土矿床的母岩属稀土元素含量较高的高 Y 轻稀土型花岗岩。风化壳矿体中的 LREE/HREE 值多介于 0.50~1.00, $Y/\Sigma REE=36\% \sim 52\%$ (湖南省核工业地质局 301 队, 2018), 显示出花岗岩母岩在经历风化作用后, 重稀土元素特别是 Y 得到了高程度的富集。对比基岩与稀土矿体的特征, 不难看出东风稀土矿床是一典型的由富轻稀土元素的母岩经风化后形成的重稀土矿床。

风化壳离子吸附型稀土矿的形成一般经历了内生作用(成矿母岩)和外生作用(风化过程)两阶段(裴秋明等, 2015; 张恋等, 2015)。东风岩体具显著的内生作用成矿: 花岗岩起源于古老地壳物质重熔, 分异指数 Di(80.38~86.95)及微量元素特征反映岩浆有一定的分离结晶作用, 矿物的显微岩相学特征则表明花岗岩内部经历了蚀变作用和重结晶作用(图 2b~f), 而结晶分异作用可促成重稀土元素的富集(张恋等, 2015), 热流体的蚀变作用(图 2e)可致黑云母等矿物减少、稀土元素矿物的形成, 从而导致稀土元素的分馏和富集(吴澄宇等, 1990; 张恋等, 2015)。总体来说, 相对南岭地区其他离子吸附型 HREE 矿床的原岩通常为高分异的花岗岩类(毛景文等, 2022), 东风岩体花岗岩的分异程度并不高, 这也与在岩体内基本未见到石英脉及细晶岩脉的地质现象相符(吴福元等, 2017)。与高分异花岗岩中较低的稀土元素含量相比, 东风岩体分异程度不高的花岗岩相对更富含稀土元素, 为后期次生富集形成稀土矿床提供了物质基础, 同时, 母岩体中的高 Y 含量更是可以形成重稀土矿床的关键。

东风岩体具有良好的外生作用成矿条件, 岩体所处地理位置为亚热带季风性湿润气候区(目前年降水量为 1500 mm 左右), 属海拔在 400~600 m、地形较缓的丘陵-低山区, 此为离子吸附型稀土矿形成的十分有利的气候和地形地貌条件(王登红等, 2013; 范飞鹏等, 2014; 裴秋明等, 2015; 张民等, 2022), 万洋山岩体和彭公庙岩体内与东风岩体地形地貌条件相似的部位也发现了一批离子吸附型稀土矿床(图 1a)。东风岩体含稀土矿风化壳具有明显的层状分带特征, 由上往下可分为腐殖层、残坡积层、全风化层和半风化层(图 3)。由腐殖层至半风化层, 伴随大气降水淋滤作用的逐渐减弱, 其 pH 值逐渐升高。在腐殖层和残坡积层中, 除 Ce 元素易由 Ce^{3+} 氧化成 Ce^{4+} 以方铈矿的形式富集于表层外(Li et al.,

2017; 王长兵等, 2021), 稀土元素(尤其为重稀土元素)在较低的 pH 值环境下迁移能力强(范飞鹏, 2014), 部分稀土元素从稀土元素矿物中分解释放出来在大气降水的淋滤作用下发生向下迁移。全风化层中随着 pH 值升高, 稀土元素迁移能力减弱, 黏土矿物对稀土元素离子的吸附能力增强, 本层以及从风化壳上部(腐殖层、残坡积层)释放迁移来的稀土元素离子大部分被黏土矿物吸附, 尤其是在表生环境中迁移能力十分强的 Y 元素(裴秋明等, 2015), 在本层得到高度富集而形成有工业价值的稀土矿体。东风矿区全风化层厚度达 10~38 m(图 3), 不仅为稀土矿的成矿作用提供了物质来源, 也提供了稀土矿体的储存空间。而半风化层中淋滤作用相对很弱, 稀土元素得不到迁移, 其品位一般与基岩相当, 不具工业价值。因此, 华南地区高钇轻稀土型母岩花岗岩在风化后可形成重稀土矿床, 在今后风化壳离子吸附型稀土矿床的找矿工作中应引起重视。

6 结 论

(1) 2 件二长花岗岩的锆石 U-Pb 定年结果分别为 (433.5 ± 2.6) Ma 和 (432.0 ± 2.5) Ma, 表明东风岩体形成于加里东晚期。

(2) 岩石主、微量元素地球化学以及锆石 Hf 同位素等特征表明, 东风岩体形成于在扬子板块与华夏板块陆内汇聚后的后碰撞伸展环境, 为增厚地壳减压熔融和软流圈地幔上涌诱发古老地壳物质重熔所形成的 S 型花岗岩。

(3) 东风稀土矿床为一由富轻稀土元素的母岩经风化后形成的重稀土矿床, 分异程度不高、富含稀土元素的高 Y 型花岗岩为矿床的形成提供了关键的物质基础, 东风岩体所处地理位置的气候及地形地貌特征为稀土元素的淋滤迁移和吸附富集提供了重要保证。

致 谢 二位匿名审稿专家对本文进行了辛勤细致的审查, 提出的宝贵意见促进了本文的进一步完善与提高, 在此表示衷心感谢。

References

- Amelin Y, Lee D C, Halliday A N and Pidgeon R T. 1999. Nature of the earth's earliest crust from hafnium isotopes in single detrital

- zircons[J]. *Nature*, 399(6733): 252-255.
- Andersrn T. 2002. Correction of common lead in U-Pb analyses that do not report ^{204}Pb [J]. *Chemical Geology*, 192: 59-79.
- Bai D Y, Huang J Z, Ma T Q and Wang X H. 2006. Geology and geochemistry of the Silurian Penggongmiao granitic pluton in the Southeastern Hunan Province and its implication for tectonic setting[J]. *Geoscience*, 20(1): 130-140(in Chinese with English abstract).
- Ballouard C, Poujol M, Boulvais P, Branquet Y, Tartèse R and Vigneresse J L. 2016. Nb-Ta fractionation in peraluminous granites: A marker of the magmatic-hydrothermal transition[J]. *Geology*, 44: 231-234.
- Bau M. 1996. Controls on the fractionation of isovalent trace elements in magmatic and aqueous systems: Evidence from Y/Ho, Zr/Hf, and lanthanide tetrad effect[J]. Contribution to Mineralogy and Petrology, 123: 323-333.
- Bea F, Mazhari A, Montero P, Amini S and Ghalamghash J. 2011. Zircon dating, Sr and Nd isotopes, and element geochemistry of the Khalifan pluton, NW Iran: Evidence for Variscan magmatism in a supposedly Cimmerian superterrane[J]. *Journal of Asian Earth Sciences*, 40: 172-179.
- Blichert-Toft J and Albarède F. 1997. The Lu-Hf isotope geochemistry of chondrites and the evolution of the mantle-crust system[J]. *Earth and Planetary Science Letters*, 148: 243-258.
- Boynton W V. 1984. Cosmochemistry of the rare earth elements: meteorites studies[A]. In: Henderson P, ed. Rare earth element geochemistry[C]. Elsevier: Amsterdam. 63-114.
- Chappell B W and White A J R. 1992. I- and S-type granites in the Lachlan Fold Belt[J]. *Transactions of the Royal Society of Edinburgh: Earth and Environmental Science*, 83: 1-26.
- Chen B F, Zou X Y, Peng L L, Qi F Y, Que X H, Zhang Q and Zhou X H. 2017. Geological characteristics and heavy Rare earth ore prospecting potential of Qingxi pluton Rare earth deposit[J]. *Chinese Rare Earths*, 40 (4): 20-31(in Chinese with English abstract).
- Chen D, Ma A J, Liu Y R and Ni Y J. 2013. Research on U-Pb chronology in Xitian pluton of Hunan Province[J]. *Geoscience*, 27(4): 819-830(in Chinese with English abstract).
- Chen D, Ma T Q, Liu W, Liu Y R, Ma A J and Ni Y J. 2016. Zircon SHRIMP U-Pb age, petrogenesis and tectonic implication of Wan-yangshan pluton in Southeast Hunan Province[J]. *Geotectonica et Metallogenesis*, 40(4): 873-890(in Chinese with English abstract).
- Chen D, Liu J Y, Wang X H, Yang J, Ma T Q and Luo L. 2017. The petrogeochemistry, SHRIMP zircon U-Pb age, and Hf isotope character of Wufengxian pluton in Hunan Province[J]. *Geological Science and Technology Information*, 36(6): 1-12(in Chinese with English abstract).
- Chen J F, Shen D, Shao Y J, Zhang J X, Liu Z F, Wei H T, Yang Q D, Luo X Y and Du Y. 2019. Silurian S-type granite-related W-(Mo) mineralization in the Nanling Range, South China: A case study of the Pingtan W-(Mo) deposit[J]. *Ore Geology Reviews*, 107: 186-200.
- Chen X M, Wang R C, Liu C S, Hu H, Zhang W L and Gao J F. 2002. Isotopic dating and genesis for Fogang biotite granites of Conghua area, Guangdong Province[J]. *Geological Journal of China Universities*, 8(3): 293-307(in Chinese with English abstract).
- Chen Z H, Li J Y, Xie P S, Zeng W and Zhou H W. 2008. Approaching the age problem for some metamorphosed Precambrian basement rocks and Phanerozoic granitic bodies in the Wuyishan area: The application of EMP monazite age dating[J]. *Geological Journal of China Universities*, 14(1): 1-15(in Chinese with English abstract).
- Cheng S B, Fu J M, Ma L Y, Chen X Q, Zhang L G and Lu Y Y. 2013. Geochemical characteristics, petrogenesis and ore potential evaluation of Caledonian granitoids in Nanling Range, South China[J]. *Geology and Mineral Resources of South China*, 29(1): 1-11(in Chinese with English abstract).
- Cheng S B, Fu J M, Ma L Y, Lu Y Y, Kou X H, Zhang L G and Huang H L. 2016. Origin of the Yuechengling caledonian granitic Batholith, northeastern Guangxi: Constraint from Zircon U-Pb geochronology, geochemistry and Nd-Hf isotopes[J]. *Geotectonica et Metallogenesis*, 40(4): 853-872(in Chinese with English abstract).
- Collins W J, Beams S D, White A J R and Chappell B W. 1982. Nature and origin of A type granites with particular reference to southeastern Australia[J]. *Contributions to Mineralogy and Petrology*, 80(2): 189-200.
- Dong G C, Mo X X, Zhao Z D, Zhu D C, Goodman R C, Kong H L and Wang S. 2013. Zircon U-Pb dating and the petrological and geochemical constraints on Lincang granite in western Yunnan, China: Implications for the closure of the Paleo-Tethys Ocean[J]. *Journal of Asian Earth Sciences*, 62: 282-294.
- Fan F P, Xiao H L, Chen L Z, Bao X M, Cai Y T, Zhang J and Zhu Y P. 2014. Mineralization and geological characteristics of elution-deposited rare earth ore from weathering crust in Pitou region, southern Ganzhou[J]. *Journal of the Chinese Society of Rare Earths*, 32(1): 101-107(in Chinese with English abstract).
- Feng Y G, Liu S W, Lü Y J, Zhang C, Shu G M and Wang C Q. 2008. Monazite age mapping of Longhua S-type granites in the northern margin of the North China Craton[J]. *Acta Petrologica Sinica*, 24 (1): 104-114(in Chinese with English abstract).
- Griffin W L, Pearson N J, Belousova E, Jackson S E, Achterherah E V, O'Reilly S Y and Shee S R. 2000. The Hf isotope composition of cratonic mantle: LA-MC-ICPMS analysis of zircon megacrysts in kimberlites[J]. *Geochimica et Cosmochimica Acta*, 64: 133-147.
- Griffin W L, Wang X, Jackson S E, Pearson N J, O'Reilly S Y, Xu X S and Zhou X M. 2002. Zircon chemistry and magma mixing, SE China: In-situ analysis of Hf isotopes, Tonglu and Pingtan igneous complexes[J]. *Lithos*, 61: 237-269.
- Griffin W L, Pearson N J, Belousova E A and Saeed A. 2006. Comment: Hf-isotope heterogeneity in zircon 91500[J]. *Chemical Geology*, 23: 358-363.
- Guo A M, Chen B H, Chen J F, Si C S and Zheng Z F. 2017. Zircon SHRIMP U-Pb geochronology of granitoids from northern Zhuangshansi granitic composite batholith, Hunan Province[J]. *Geo-*

- logy in China, 44(4): 781-792 (in Chinese with English abstract).
- Hoskin P W O and Schaltegger U. 2003. The composition of zircon and igneous and metamorphic petrogenesis[J]. *Reviews of Mineralogy and Geochemistry*, 53: 27-62.
- Hu Z C, Liu Y S, Gao S, Liu W G, Zhang W, Tong X R, Lin L, Zong K Q, Li M, Chen H H, Zhou L and Yang L. 2012. Improved in situ Hf isotope ratio analysis of zircon using newly designed X Skinner cone and jet sample cone in combination with the addition of nitrogen by laser ablation multiple collector ICP-MS[J]. *Journal of Analytical Atomic Spectrometry*, 27: 1391-1399.
- Hunan Institute of Geological Survey. 1972. 1: 200 000 Yongxing regional geological survey report[R]. 1-112(in Chinese).
- Hunan Institute of Geological Survey. 2005. 1: 250 000 Hengyang regional geological survey report[R]. 1-324(in Chinese).
- Hunan Institute of Geological Survey. 2014. Regional geology and mineral resources prospect survey report in Chaling-Ninggang district, Hunan[R]. 1-149(in Chinese).
- Hunan Institute of Geological Survey. 2018. 1:50 000 Regional geology and mineral resources survey report in Huanxi district, Hunan[R]. 1-236(in Chinese).
- Le Bas M J, Le Maître R W, Streckeisen A and Zanettin B. 1986. A chemical classification of volcanic rocks based on the total alkali-silica system[J]. *Journal of Petrology*, 27: 745-750.
- Li C N. 1992. Trace element in igneous rock[M]. Wuhan: China University of Geosciences. 1-187(in Chinese).
- Li J K, Chen Z Y, Chen Z H, Hou K J and Zhao Z. 2012. The dating and analysis of ore-forming conditions for Hanfang granite intrusions in Ganxian, Jiangxi Province[J]. *Rock and Mineral Analysis*, 31(4): 717-723 (in Chinese with English abstract).
- Li T, Yuan H Y and Wu S X. 1998. On the average chemical composition of granitoids in China and the world[J]. *Geotectonica et Metallogenesis*, 22(1): 29-34 (in Chinese with English abstract).
- Li X H, Chen Z G, Liu D Y and Li W X. 2003. Jurassic gabbro-granite-syenite suites from southern Jiangxi Province, SE China: Age, origin, and tectonic significance[J]. *International Geology Review*, 45: 898-921.
- Li Y H M, Zhao W W and Zhou M F. 2017. Nature of parent rocks, mineralization styles and ore genesis of regolith-hosted REE deposits in South China: An integrated genetic model[J]. *Journal of Asian Earth Sciences*, 148: 65-95.
- Li Z X, Li X H, Wartho J A, Clark C, Li W X and Zhang C L. 2010. Magmatic and metamorphic events during the Early Paleozoic Wuyi-Yunkai orogeny, southeastern South China: New age constraints and pressure-temperature conditions[J]. *Geological Society of America Bulletin*, 122(5-6): 772-793.
- Liang X Q, Dong C G, Jiang Y, Wu S C, Zhou Y, Zhu H F, Fu J G, Wang C and Shan Y H. 2016. Zircon U-Pb, molybdenite Re-Os and muscovite Ar-Ar isotopic dating of the Xitian W-Sn polymetallic deposit, eastern Hunan Province, South China and its geological significance[J]. *Ore Geology Reviews*, 78: 85-100.
- Liu Y S, Hu Z C, Gao S, Günther D, Xu J, Gao C G and Chen H H. 2008. In situ analysis of major and trace elements of anhydrous minerals by LA-ICP-MS without applying an internal standard[J]. *Chemical Geology*, 257: 34-43.
- Liu Y S, Gao S, Hu Z C, Gao C G, Zong K Q and Wang D B. 2010. Continental and oceanic crust recycling-induced melt-peridotite interactions in the Trans-North China Orogen: U-Pb dating, Hf isotopes and trace elements in zircons of mantle xenoliths[J]. *Journal of Petrology*, 51 (1-2): 537-571.
- Ludwig K R. 2003. ISOPLOT 3.00: A Geochronological Toolkit for Microsoft Excel[M]. Berkeley Geochronology Center, California, Berkeley: 39.
- Ma T Q, Bai D Y, Kuang J and Wang X H. 2005. Zircon SHRIMP dating of the Xitian granite pluton, Chaling southeastern Hunan, and its geological significance[J]. *Geological Bulletin of China*, 24(5): 415-419 (in Chinese with English abstract).
- Maniar P D and Piccoli P M. 1989. Tectonic discrimination of granitoids[J]. *Geological Society of America Bulletin*, 101: 635-643.
- Mao J W, Song S W, Liu M and Meng J Y. 2022. REE deposits: Basic characteristics and global metallogeny[J]. *Acta Geologica Sinica*, 96(11): 3675-36972 (in Chinese with English abstract).
- Niu R, Liu Q, Hou Q L, Sun J F, Wu S C and Zhang H Y, Guo Q Q and Wang Q. 2015. Zircon U-Pb geochronology of Xitian granitic pluton in Hunan Province and its constraints on the metallogenic ages of the tungsten-tin deposit[J]. *Acta Petrologica Sinica*, 31(9): 2620-2632 (in Chinese with English abstract).
- No.301 Brigade of Hunan Nuclear Geological Bureau. 2018. General investigation geological report of Dongfeng REE deposit in Yanling Country, Hunan Province[R]. 1-71 (in Chinese).
- Patino D A E and Johnston A D. 1991. Phase equilibria and melt productivity in the pelitic system: Implications for the origin of per-aluminous granitoids and aluminous granites[J]. *Contributions to Mineralogy and Petrology*, 107: 202-218.
- Patino D A E and Beard J S. 1995. Dehydration-melting of biotite-granite and quartz amphibolite from 3 to 15 Kbar[J]. *Journal of Petrology*, 36: 707-738.
- Pearce J A, Harris N B W and Tindle A G. 1984. Trace element discrimination diagrams for the tectonic interpretation of granitic rocks[J]. *Journal of Petrology*, 25(4): 956-983.
- Pearce J A. 1996. Sources and settings of granitic rocks[J]. *Episodes*, 19: 120-125.
- Pei Q M, Liu T Q, Yuan H Q, Cao H W, Li S H and Hu X K. 2015. Geochemical characteristics of trace elements of ion adsorption type rare elements deposit in Guposhan region, Guangxi, China[J]. *Journal of Chengdu University of Technology(science and technology edition)*, 42(4): 451-462 (in Chinese with English abstract).
- Ren F, Yin F G, Xu B, Liu H L, Fan B L, Xu C H, and Bai J G. 2021. Zircon U-Pb age and Hf isotope of Early Paleozoic granite from the Jitang area in eastern Tibet and its insight into the evolution of the evolution of the Proto-Tethys Ocean[J]. *Geological Bulletin of China*, 40(11): 1865-1876 (in Chinese with English abstract).
- Rollinson H R. 1993. Using geochemical data: Evaluation, presenta-

- tion, interpretation[M]. New York: Longman Scientific & Technical. 1-352.
- Segal I, Halicz L and Platzner I T. 2003. Accurate isotope ratio measurements of ytterbium by multiple collection inductively coupled plasma mass spectrometry applying erbium and hafnium in an improved double external normalization procedure[J]. *Journal of Analytical Atomic Spectrometry*, 18: 1217-1223.
- Shen W Z, Zhang F R, Shu L S, Wang L J and Xiang L. 2008. Formation age, geochemical characteristics of the Ninggang granite body in Jiangxi Province and its tectonic significance[J]. *Acta Petrologica Sinica*, 24(10): 2244-2254(in Chinese with English abstract).
- Shu L S. 2006. Predevonian tectonic evolution of South China: From Cathaysian Block to Caledonian period folded orogenic Belt[J]. *Geological Journal of China Universities*, 12(4): 418-431(in Chinese with English abstract).
- Shu L S, Yu J H, Jia D, Wang B, Shen W Z and Zhang Y Q. 2008. Early Paleozoic orogenic belt in the eastern segment of South China[J]. *Geological Bulletin of China*, 27(10): 1581-1593(in Chinese with English abstract).
- Soderlund U, Patchett P J, Vervoort J D and Isachsen C E. 2004. The ^{176}Lu decay constant determined by Lu-Hf and U-Pb isotope systematics of Precambrian mafic intrusions[J]. *Earth and Planetary Science Letters*, 219: 311-324.
- Su X Y, Guo C L, Chen Z Y, Zhao Z, Guo N X and Zhao Z. 2014. Zircon U-Pb age, geochemistry and mineralization prospective of the Caledonian Doushui granitic pluton in southern Jiangxi Province[J]. *Geotectonica et Metallogenesis*, 38(2): 334-346(in Chinese with English abstract).
- Sun S S and McDonough W F. 1989. Chemical and isotopic systematics of oceanic basalts: Implications for mantle composition and processes[J]. Geological Society, London, Special Publications, 42: 313-345.
- Sun Y, Li J K, Chen Z Y, Chen Z H, Hou K J and Zhao Z. 2012. LA-MC-ICP-MS Zircon U-Pb dating and rare earth potential of the Longshe granite in Ganzhou, Jiangxi Province[J]. *Geotectonica et Metallogenesis*, 36(3): 422-426(in Chinese with English abstract).
- The Granitoid Resrarch Group of the Nanling Project, MGMR. 1989. Geology of granitoids of Nanling region and their petrogenesis and mineralization[M]. Beijing: Geological Publishing House. 1-437(in Chinese with English abstract).
- Vervoort J D, Pachelt P J, Gehrels G E and Nutman A P. 1996. Constraints on Early Earth differentiation from hafnium and neodymium isotopes[J]. *Nature*, 379: 624-627.
- Wan Y S, Liu D Y, Wilde S A, Cao J J, Chen B, Dong C Y, Song B and Du L L. 2010. Evolution of the Yunkai Terrane, South China: Evidence from SHRIMP zircon U-Pb dating, geochemistry and Nd isotope[J]. *Journal of Asian Earth Sciences*, 37(2): 140-153.
- Wang C B, Ni G Q, Qu L, Wu R L, Li C Q, Ma X, Zhang Z J and Yang C P. 2021. Ce geochemical characteristics of granite weathering crust and its prospecting significance: A case study of Chahe ion adsorption rare earth deposit in western Yunnan[J]. *Mineral Deposits*, 40(5): 1013-1028(in Chinese with English abstract).
- Wang D H, Zhao Z, Yu Y, Zhao T, Li J K, Dai J J, Liu X X and He H H. 2013. Progress, problems and research orientation of ion-adsorption type rare earth resources[J]. *Rock and Mineral Analysis*, 32(5): 796-802(in Chinese with English abstract).
- Wang D H, Zhao Z, Yu Y, Wang C H, Da J J, Sun Y Zhao T, Li J K, Huang F, Chen Z Y, Zeng Z L, Deng M C, Zou X Y, Huang H G, Zhou H and Feng W J. 2017. A review of the achievements in the survey and study of ion-adsorption type REE deposits in China[J]. *Acta Geoscientica Sinica*, 38(3): 317-325(in Chinese with English abstract).
- Wang T and Liu S. 2013. Zircon saturation temperatures of granites in the Jiaonan area and their geological significations[J]. *Bulletin of Mineralogy, Petrology and Geochemistry*, 32(5): 619-624(in Chinese with English abstract).
- Wang Y B, Wang D H, Han J, Chen Z H and Wang Q L. 2010. U-Pb dating and Hf isotopic characteristics of zircons from quartz-diorite in the Yijiang REE-Sc deposit, Rucheng County, Hunan: Constraints on the timing of Caledonian magmatic activity in South China[J]. *Geology in China*, 37(4): 1062-1070(in Chinese with English abstract).
- Wang Y J, Fan W M, Sun M, Liang X Q, Zhang Y H and Peng T P. 2007a. Geochronological, geochemical and geothermal constraints on petrogenesis of the the Indosinian peraluminous granites in the South China Block: A case study in the Hunan Province[J]. *Lithos*, 96(3): 475-502.
- Wang Y J, Fan W M, Zhao G C, Ji S C and Peng T P. 2007b. Zircon U-Pb geochronology of gneissic rocks in the Yunkai Massif and its implications on the Caledonian event in the South China Block[J]. *Gondwana Research*, 12(4): 404-416.
- Wang Y J, Zhang F F, Fan W M, Zhang G W, Chen S Y, Peter A C and Zhang A M. 2010. Tectonic setting of the South China Block in the Early Paleozoic: Resolving intracontinental and ocean closure models from detrital zircon U-Pb geochronology[J]. *Tectonics*, 29, doi: 10.1029/2010TC002750.
- Watson E B and Harrison T M. 1983. Zircon saturation revisited: Temperature and composition effects in a variety of crustal magma types[J]. *Earth and Planetary Science Letters*, 64: 295-304.
- Whalen J B, Currie K L and Chappell B W. 1987. A-type granites: Geochemical characteristics, discrimination and petrogenesis[J]. *Contributions to Mineralogy and Petrology*, 95: 407-419.
- Wu C Y, Huang D H, Bai G and Ding X S. 1990. Differentiation of Rare earth elements and origin of granitic rocks, Nanling Mountain area[J]. *Acta Petrologica et Mineralogica*, 9(2): 106-117(in Chinese with English abstract).
- Wu F Y, Yang Y H, Xie L W, Yang J H and Xu P. 2006. Hf isotopic compositions of the standard zircons and baddeleyites used in U-Pb geochronology[J]. *Chemical Geology*, 234: 105-126.
- Wu F Y, Li X H, Zheng Y F and Gao S. 2007. Lu-Hf isotopic systematics and their applications in petrology[J]. *Acta Petrologica Sinica*,

- 23(2): 185-220(in Chinese with English abstract).
- Wu F Y, Liu X C, Ji W Q, Wang J M and Yang L. 2017. Highly fractionated granites: Recognition and research[J]. *Science China Earth Sciences*, 60: 1201-1219(in Chinese).
- Wu G Y, Ma T Q, Feng Y F, Yan Q R, Liu F G and Bai D Y. 2008. Geological and geochemical characteristics and genesis of the Caledonian Wanyangshan granite in the Nanling Mountains, South China[J]. *Geology in China*, 35(4): 608-617(in Chinese with English abstract).
- Wu Q H, Cao J Y, Kong H, Shao Y J, Li H, Xi X S and Deng X T. 2016. Petrogenesis and tectonic setting of the Early Mesozoic Xitian granitic pluton in the middle Qin-Hang Belt, South China: Constraints from zircon U-Pb ages and bulk-rock trace element and Sr-Nd-Pb isotopic compositions[J]. *Journal of Asian Earth Sciences*, 128: 130-148.
- Wu Y B and Zheng Y F. 2004. Genesis of zircon and its constraints on interpretation of U-Pb age[J]. *Chinese Science Bulletin*, 49(16): 1589-1604(in Chinese).
- Xu X, O'Reilly S Y, Griffin W L, Wang X, Pearson N J and He Z. 2007. The crust of Cathaysia: Age, assembly and reworking of two terranes[J]. *Precambrian Research*, 158(1-2): 51-78.
- Xu X B, Zhang Y Q, Shu L S, Jia D, Wang R R and Xu H Z. 2009. Zircon La-ICPMS U-Pb dating of the Weipu granitic pluton in Southwest Fujian and the Changpu migmatite in South Jiangxi: Constraints to the timing of Caledonian movement in Wuyi mountains[J]. *Geology Review*, 55(2): 277-285(in Chinese with English abstract).
- Yao Y, Chen J, Lu J J and Zhang R Q. 2013. Geochronology, Hf isotopic compositions and geochemical characteristics of Xitian A-type granite and its geological significance[J]. *Mineral Deposits*, 32(3): 467-488(in Chinese with English abstract).
- Yu J H, O'Reilly S Y, Wang L, Griffin W L, Zhou M F, Zhang M and Shu L. 2010. Components and episodic growth of Precambrian crust in the Cathaysia Block, South China: Evidence from U-Pb ages and Hf isotopes of zircons in Neoproterozoic sediments[J]. *Precambrian Research*, 181(1-4): 97-114.
- Yu Y, Chen Z Y, Chen Z H, Hou K J, Zhao Z, Xu J X, Zhang J J and Zeng Z L. 2012. Zircon U-Pb dating and mineralization prospective of the Triassic Qingxi Pluton in southern Jiangxi Province[J]. *Geotectonica et Metallogenesis*, 36(3): 413-421(in Chinese with English abstract).
- Zhang A M, Wang Y J, Fan W M, Zhang F F and Zhang Y Z. 2010. LA-ICPMS zircon U-Pb geochronology and Hf isotopic compositions of Caledonian granites from the Qingliu area, Southwest Fujian[J]. *Geotectonica et Metallogenesis*, 38(3): 408-418(in Chinese with English abstract).
- Zhang F F, Wang Y J, Fan W M, Zhang A M and Zhang Y Z. 2010. LA-ICPMS zircon U-Pb geochronology of Late Early Paleozoic granites in eastern Hunan and western Jiangxi Province, South China[J]. *Geochimica*, 39(5): 414-426 (in Chinese with English abstract).
- Zhang F R, Shu L S, Wang D Z, Yu J H and Shen W Z. 2009. Discussions on the tectonic setting of Caledonian granitoids in the eastern segment of South China[J]. *Earth Science Frontiers*, 16(1): 248-260 (in Chinese with English abstract).
- Zhang L, Wu K X, Chen L K, Zhu P and Ouyang H. 2015. Overview of metallogenic features of ion-adsorption type REE deposits in southern Jiangxi Province[J]. *Journal of the Chinese Society of Rare Earths*, 33(1): 10-17(in Chinese with English abstract).
- Zhang M, Tan W, He X C, Zhao F F and Luo L Y. 2022. Analysis on geological characteristics and discussion about metallogenic process for ion-adsorption type REE deposit in Lancang County, Yunnan Province[J]. *Mineral Deposits*, 41(3): 567-584(in Chinese with English abstract).
- Zhang Q, Zhai M G, Wei C J, Zhou L G, Chen W F, Jiao S T, Wang Y and Yuan F L. 2022. Innovative petrogenetic classification of granitoids: Perspective from metamorphic anatexis and big data[J]. *Earth Science Frontiers*, 29(4): 319-329(in Chinese with English abstract).
- Zhang W L, Wang R C, Lei Z H, Hua R M, Zhu J C, Lu J J, Xie L, Che X D, Zhang R Q, Yao Y and Chen J. 2011. Zircon U-Pb dating confirms existence of a Caledonian scheelite bearing aplitic vein in the Penggongmiao granite batholith, South Hunan[J]. *Chinese Science Bulletin*, 56: 1448-1454(in Chinese).
- Zhao K D, Jiang S Y, Sun T, Chen W F, Ling H F and Chen P R. 2013. Zircon U-Pb dating, trace element and Sr-Nd-Hf isotope geochemistry of Paleozoic granites in the Miao'ershan-Yuechengling batholith, South China: Implication for petrogenesis and tectonic-magmatic evolution[J]. *Journal of Asian Earth Sciences*, 74: 244-264.
- Zhao Z, Chen Z Y, Chen Z H, Hou K J, Zhao Z, Xu J X, Zhang J J and Zeng Z L. 2012. Zircon U-Pb dating, tectonic setting and ore-bearing properties evaluation of the Caledonian Yangbu pluton in South Jiangxi[J]. *Rock and Mineral Analysis*, 31(3): 530-535(in Chinese with English abstract).
- Zhao Z, Wang D H, Chen Z Y, Guo N X, Liu X X and He H H. 2014. Metallogenic specialization of rare earth mineralized igneous rocks in the eastern Nanling Region[J]. *Geotectonica et Metallogenesis*, 38(2): 255-263(in Chinese with English abstract).
- Zhao Z, Wang D H and Zou X Y. 2022. The genesis and diversity of ion adsorption REE mineralization in the Zhaibei deposit, Jiangxi Province, South China[J]. *Acta Petrologica Sinica*, 38(2): 365-370 (in Chinese with English abstract).
- Zheng G D, Li J K, Chen Z Y, Chen Z H, Hou K J and Zhao Z. 2012. U-Pb dating of zircon from Jibu Huangsha intrusions in southern Jiangxi Province and its geological significances[J]. *Rock and Mineral Analysis*, 31(4): 711-716(in Chinese with English abstract).
- Zhou M F, Li X X, Wang Z C, Li X C and Liu J C. 2020. The genesis of regolith-hosted rare earth element and scandium deposits: Current understanding and outlook to future prospecting[J]. *Chinese Science Bulletin*, 65(33): 3809-3824(in Chinese).
- Zhou Y, Liang X Q, Wu S C, Jiang Y, Wen S N and Cai Y F. 2013. Geo-

- chronology and geochemical characteristics of the Xitian tungsten-tin-bearing A-type granites, Hunan Province, China[J]. Geotectonica et Metallogenica, 37(3): 511-529(in Chinese with English abstract).
- Zhou Y, Liang X Q, Wu S C, Cai Y F, Liang X R, Shao T B, Wang C, Fu J G and Ying J. 2015. Isotopic geochemistry, zircon U-Pb ages and Hf isotopes of A-type granites from the Xitian W-Sn deposit, SE China: Constraints on petrogenesis and tectonic significance[J]. Journal of Asian Earth Sciences, 105: 122-139.
- ### 附中文参考文献
- 柏道远,黄建中,马铁球,王先辉.2006.湘东南志留纪彭公庙花岗岩体的地质地球化学特征及构造背景[J].现代地质,20(1): 130-140.
- 陈斌锋,邹新勇,彭琳琳,漆富勇,阙兴华,张青,周兴华.2019.清溪岩体稀土矿床地质特征及重稀土找矿潜力[J].稀土,40(4): 20-31.
- 陈迪,马爱军,刘伟,刘耀荣,倪艳军.2013.湖南锡田花岗岩体锆石U-Pb年代学研究[J].现代地质,27(4): 819-830.
- 陈迪,马铁球,刘伟,刘耀荣,马爱军,倪艳军.2016.湘东南万洋山岩体的锆石SHRIMP U-Pb年龄、成因及构造意义[J].大地构造与成矿,40(4): 873-890.
- 陈迪,刘珏懿,王先辉,杨俊,马铁球,罗来.2017.湖南五峰仙岩体岩石地球化学、SHRIMP U-Pb年龄及Hf同位素特征[J].地质科技情报,36(6): 1-12.
- 陈小明,王汝成,刘昌实,胡欢,张文兰,高剑锋.2002.广东从化佛冈(主体)黑云母花岗岩定年和成因[J].高校地质学报,8(3): 293-307.
- 陈正宏,李寄嶠,谢佩姗,曾雯,周汉文.2008.利用EMP独居石定年法探讨浙闽武夷山地区变质基底岩石与花岗岩的年龄[J].高校地质学报,14(1): 1-15.
- 程顺波,付建明,马丽艳,陈希清,张利国,卢友月.2013.南岭地区加里东期花岗岩地球化学特征、岩石成因及含矿性评价[J].华南地质与矿产,29(1): 1-11.
- 程顺波,付建明,马丽艳,卢友月,寇晓虎,张利国,黄惠兰.2016.桂东北越城岭岩体加里东期成岩作用:锆石U-Pb年代学、地球化学和Nd-Hf同位素制约[J].大地构造与成矿学,40(4): 853-872.
- 地矿部南岭项目花岗岩专题组.1989.南岭花岗岩地质及其成因和成矿作用[M].北京:地质出版社.1-437.
- 范飞鹏,肖惠良,陈乐柱,鲍晓明,蔡逸涛,张洁,朱意萍.2014.赣南陂头一带风化壳淋积型稀土矿成矿地质特征[J].中国稀土学报,32(1): 101-107.
- 凤永刚,刘树文,吕勇军,张臣,舒桂明,王长秋.2008.华北克拉通边缘隆化地区S型花岗岩的独居石年龄图谱[J].岩石学报,24(1): 104-114.
- 郭爱民,陈必河,陈剑锋,司程山,郑正福.2017.南岭诸广山北体复合花岗岩锆石SHRIMP U-Pb定年及地质意义[J].中国地质,44(4): 781-792.
- 湖南省地质调查院.1972.1:20万永兴幅区域地质报告[R].1-112.
- 湖南省地质调查院.2005.1:25万衡阳市幅区域地质调查报告[R].1-324.
- 湖南省地质调查院.2014.湖南茶陵-宁岗地区矿产远景调查成果报告[R].1-149.
- 湖南省地质调查院.2018.湖南浣溪地区1:5万地质矿产综合调查成果报告[R].1-236.
- 湖南省核工业地质局三〇一大队.2018.湖南省炎陵县东风矿区稀土矿普查地质报告[R].1-71.
- 黎彤,袁怀雨,吴胜昔.1998.中国花岗岩类和世界花岗岩类平均化学成分的对比研究[J].大地构造与成矿学,22(1): 29-34.
- 李昌年.1992.火成岩微量元素岩石学[M].武汉:中国地质大学出版社.1-187.
- 李建康,陈振宇,陈郑辉,侯可军,赵正.2012.江西赣县韩坊岩体的成岩时代及成矿条件分析[J].岩矿测试,31(4): 717-723.
- 马铁球,柏道远,邝军,王先辉.2005.湘东南茶陵地区锡田岩体锆石SHRIMP定年及其地质意义[J].地质通报,24(5): 415-419.
- 毛景文,宋世伟,刘敏,孟健寅.2022.稀土矿床:基本特点与全球分布规律[J].地质学报,96(11): 3675-3697.
- 牛睿,刘庆,侯泉林,孙金凤,伍式崇,张宏远,郭谦谦,王麒.2015.湖南锡田花岗岩锆石U-Pb年代学及钨锡成矿时代的探讨[J].岩石学报,31(9): 2620-2632.
- 裴秋明,刘图强,苑鸿庆,曹华文,李社宏,胡昕凯.2015.广西姑婆山离子吸附型稀土矿床微量元素地球化学特征[J].成都理工大学学报(自然科学版),42(4): 451-462.
- 任飞,尹福光,徐波,刘恒麟,樊炳良,徐长昊,白景国.2021.藏东吉塘地区早古生代花岗岩锆石U-Pb年龄、Hf同位素及其对原特提斯洋演化的启示[J].地质通报,40(11): 1865-1876.
- 沈渭洲,张芳荣,舒良树,王丽娟,向磊.2008.江西宁冈岩体的形成时代、地球化学特征及其构造意义[J].岩石学报,24(10): 2244-2254.
- 舒良树.2006.华南前泥盆纪构造演化:从华夏地块到加里东期造山带[J].高校地质学报,12(4): 418-431.
- 舒良树,于津海,贾东,王博,沈渭洲,张岳桥.2008.华南东段早古生代造山带研究[J].地质通报,27(10): 1581-1593.
- 苏晓云,郭春丽,陈振宇,赵正,郭娜欣,赵芝.2014.赣南加里东期陡水岩体的锆石U-Pb年龄、地球化学特征及其稀土含矿性探讨[J].大地构造与成矿学,38(2): 334-346.
- 孙艳,李建康,陈振宇,陈郑辉,侯可军,赵正.2012.江西新丰桐木稀土矿区龙舌岩体的成矿时代及成矿条件分析[J].大地构造与成矿学,36(3): 422-426.
- 王长兵,倪光清,瞿亮,伍荣林,李灿清,马鑫,张子军,杨春鹏.2021.花岗岩风化壳中Ce地球化学特征及其找矿意义——以滇西岔河离子吸附型稀土矿床为例[J].矿床地质,40(5): 1013-1028.
- 王登红,赵芝,于扬,赵汀,李建康,代晶晶,刘新星,何哈哈.2013.离子吸附型稀土资源研究进展、存在问题及今后研究方向[J].岩石学报,32(5): 796-802.
- 王登红,赵芝,于扬,王成辉,代晶晶,孙艳,赵汀,李建康,黄凡,陈振宇,曾载淋,邓茂春,邹新勇,黄华谷,周辉,冯文杰.2017.我国离子吸附型稀土矿产科学的研究和调查评价新进展[J].地球学报,38(3): 317-325.
- 王涛,刘燊.2013.赣南花岗岩锆石饱和温度及其地质意义[J].矿物岩石地球化学通报,32(5): 619-624.
- 王彦斌,王登红,韩娟,陈郑辉,王清利.2010.湖南益将稀土-钪矿的

- 石英闪长岩锆石 U-Pb 定年和 Hf 同位素特征: 湘南加里东期岩浆活动的年代学证据[J]. 中国地质, 37(4): 1062-1070.
- 吴澄宇, 黄典豪, 白鸽, 丁孝石. 1990. 南岭花岗岩类起源与稀土元素的分馏[J]. 岩石矿物学杂志, 9(2): 106-117.
- 吴福元, 李献华, 郑永飞, 高山. 2007. Lu-Hf 同位素体系及其岩石学应用[J]. 岩石学报, 23(2): 185-220.
- 吴福元, 刘小驰, 纪伟强, 王佳敏, 杨雷. 2017. 高分异花岗岩的识别与研究[J]. 中国科学: 地球科学, 47: 745-765
- 吴元保, 郑永飞. 2004. 锆石成因矿物学研究及其对 U-Pb 年龄解释的制约[J]. 科学通报, 49(16): 1589-1604.
- 伍光英, 马铁球, 冯艳芳, 闫全人, 刘富国, 柏道远. 2008. 南岭万洋山加里东期花岗岩地质地球化学特征及其成因[J]. 中国地质, 35(4): 608-617.
- 徐先兵, 张岳桥, 舒良树, 贾东, 王瑞瑞, 许怀智. 2009. 闽西南玮埔岩体和赣南菖蒲混合锆石 LA-ICPMS U-Pb 年代学: 对武夷山加里东运动时代的制约[J]. 地质论评, 55(2): 277-285.
- 姚远, 陈骏, 陆建军, 章荣清. 2013. 湘东锡田 A 型花岗岩的年代学、Hf 同位素、地球化学特征及其地质意义[J]. 矿床地质, 32(3): 467-488.
- 于扬, 陈振宇, 陈郑辉, 侯可军, 赵正, 许建祥, 张家菁, 曾载淋. 2012. 赣南印支期清溪岩体的锆石 U-Pb 年代学研究及其含矿性评价[J]. 大地构造与成矿学, 36(3): 413-421.
- 张爱梅, 王岳军, 范蔚茗, 张菲菲, 张玉芝. 2010. 闽西南清流地区加里东期花岗岩锆石 U-Pb 年代学及 Hf 同位素组成研究[J]. 大地构造与成矿学, 34(3): 408-418.
- 张芳荣, 舒良树, 王德滋, 于津海, 沈渭洲. 2009. 华南东段加里东期花岗岩类形成构造背景探讨[J]. 地学前缘, 16(1): 248-260.
- 张菲菲, 王岳军, 范蔚茗, 张爱梅, 张玉芝. 2010. 湘东-赣西地区早古生代晚期花岗岩的 LA-ICPMS 锆石 U-Pb 定年研究[J]. 地球化学, 39(5): 414-426.
- 张恋, 吴开兴, 陈陵康, 朱平, 欧阳杯. 2015. 赣南离子吸附型稀土矿床成矿特征概述[J]. 中国稀土学报, 33(1): 10-17.
- 张民, 谭伟, 何显川, 赵甫峰, 罗莲英. 2022. 云南省澜沧县离子吸附型稀土矿床地质特征分析与成矿过程探讨[J]. 矿床地质, 41(3): 567-584.
- 张旗, 翟明国, 魏春景, 周李岗, 陈万峰, 焦守涛, 王跃, 袁方林. 2022. 一个新的花岗岩成因分类: 基于变质岩深熔作用理论与大数据的证据[J]. 地学前缘, 29(4): 319-329.
- 张文兰, 王汝成, 雷泽恒, 华仁民, 朱金初, 陆建军, 谢磊, 车旭东, 章荣清, 姚远, 陈骏. 2011. 湘南彭公庙加里东期含白钨矿细晶岩脉的发现[J]. 科学通报, 56: 1448-1454.
- 赵芝, 陈振宇, 陈郑辉, 侯可军, 赵正, 许建祥, 张家菁, 曾载淋. 2012. 赣南加里东期阳埠(堰子下)岩体的锆石年龄、构造背景及其含矿性评价[J]. 岩矿测试, 31(3): 530-535.
- 赵芝, 王登红, 陈振宇, 郭娜欣, 刘新星, 何晗晗. 2014. 南岭东段与稀土矿有关岩浆岩的成矿专属性特征[J]. 大地构造与成矿学, 38(2): 255-263.
- 赵芝, 王登红, 邹新勇. 2022. “寨背式”离子吸附型稀土矿床多类型稀土矿化及其成因[J]. 岩石学报, 38(2): 356-370.
- 郑国栋, 李建康, 陈振宇, 陈郑辉, 侯可军, 赵芝. 2012. 赣南吉埠黄沙岩体的锆石 U-Pb 法年代学研究及其他地质意义[J]. 岩矿测试, 31(4): 711-716.
- 周美夫, 李欣禧, 王振朝, 李晓春, 刘嘉成. 2020. 风化壳型稀土和钪矿床成矿过程的研究进展和展望[J]. 科学通报, 65(33): 3809-3824.
- 周云, 梁新权, 梁细荣, 伍式崇, 蒋英, 温淑女, 蔡永丰. 2013. 湖南锡田含 W-Sn A 型花岗岩年代学与地球化学特征[J]. 大地构造与成矿学, 37(3): 511-529.